A&A 430, 255–262 (2005)
DOI: 10.1051/0004-6361:20041540

Astronomy & Astrophysics

Thorium-rich halo star HD 221170: Further evidence against the universality of the r-process⋆,⋆⋆

A. Yushchenko[1,2], V. Gopka[2], S. Goriely[3], F. Musaev[4,5,6], A. Shavrina[7], C. Kim[8], Y. Woon Kang[1], J. Kuznietsova[5,7], and V. Yushchenko[9]

[1] Astrophysical Research Center for the Structure and Evolution of the Cosmos (ARCSEC), Sejong University, Seoul 143-747, Korea
e-mail: yua@arcsec.sejong.ac.kr; kangyw@sejong.ac.kr
[2] Odessa Astronomical observatory, Odessa National University, Park Shevchenko, Odessa 65014, Ukraine
e-mail: yua@odessa.net; gopka@arctur.tenet.odessa.ua
[3] Institut d'Astronomie et d'Astrophysique, Université Libre de Bruxelles, CP 226, 1050 Brussels, Belgium
e-mail: sgoriely@astro.ulb.ac.be
[4] Special Astrophysical observatory of the Russian Academy of Sciences, Nizhnij Arkhyz, Zelenchuk, Karachaevo-Cherkesiya 369167, Russia
e-mail: faig@sao.ru
[5] The International Centre for Astronomical, Medical and Ecological Research of the Russian Academy of Sciences and the National Academy of Sciences of Ukraine, Golosiiv, Kiev 03680, Ukraine
e-mail: admin@terskol.com
[6] Shamakhy Astrophysical Observatory, NAS of Azerbaijan, Yusif Mamedaliev, Shamakhy, Azerbaijan
[7] Main Astronomical observatory, NAS of Ukraine, Kiiv 03680, Ukraine
e-mail: shavrina@mao.kiev.ua
[8] Department of Earth Science Education, Chonbuk National University, Chonju 561-756, Korea
e-mail: chkim@astro.chonbuk.ac.kr
[9] Odessa National University, Odessa 65014, Ukraine
e-mail: yushchenko@mail.ru

Received 4 March 2004 / Accepted 8 September 2004

Abstract. We report the abundance determination in the atmosphere of the bright halo star HD 221170. The spectra were taken with the Terskol Observatory's 2.0-m telescope with a resolution R = 45 000 and signal-to-noise ratio up to 250 in the wavelength region 3638–10 275 Å. The adopted atmospheric parameters correspond to an effective temperature $T_{\rm eff}$ = 4475 K, a surface gravity log g = 1.0, a microturbulent velocity $\upsilon_{\rm micro}$ = 1.7 km s^{-1}, and a macroturbulent velocity $\upsilon_{\rm macro}$ = 4 km s^{-1}. The abundances of 43 chemical elements were determined with the method of spectrum synthesis. The large overabundances (by 1 dex relative to iron) of elements with $Z > 38$ are shown to follow the same pattern as the solar r-abundances. The present HD 221170 analysis confirms the non-universality of the r-process, or more exactly the observation that the astrophysical sites hosting the r-process do not always lead to a unique relative abundance distribution for the bulk Ba to Hg elements, the Pb-peak elements, and the actinides.

Key words. line: identification – stars: abundances – stars: atmospheres – stars: evolution – stars: individual: HD 221170 – nuclear reactions, nucleosynthesis, abundances

1. Introduction

The chemical composition of different objects, particularly halo stars, is one of the most important clues for understanding the structure and evolution of the Universe. Typical investigations of the chemical compositions of stars usually show 15–40 chemical elements, depending the type of the star. The most detailed stellar abundance patterns consist of 50–58 elements (see Yushchenko et al. 2004, for examples). The best example is the abundance pattern of the halo star CS22892-52 with the determination of 58 elements (Sneden et al. 2003). This star and another three r-process-rich stars CS31082-001 (Cayrel et al. 2001; Hill et al. 2002), HD 115444 (Westin et al. 2000) and BD+17°3248 (Cowan et al. 2002) are halo stars with known enhanced abundances of

⋆ Based on observations obtained at the 2-m telescope of Peak Terskol observatory, International Center for Astronomical, Medical and Ecological Research, Ukraine & Russia.
⋆⋆ Tables 1 and 2 are only available in electronic form at http://www.edpsciences.org

thorium with respect to iron. In the specific case of CS31082-001, the determination of the uranium abundance also enabled investigators to derive from the thorium to uranium abundance ratio a stellar age of 13 ± 4 billion years. Such an estimate directly provides an independent lower limit for the age of our Galaxy and the Universe.

The investigation of the thorium abundance in the atmosphere of different stars of our Galaxy has a long history. Bucher (1987), Morel et al. (1992) and Francois et al. (1993) studied a set of disk and halo stars using the strongest Th line at 4019.129 Å. Yushchenko & Gopka (1994) determined the thorium abundance in Procyon using 4 faint lines in the 3200–3500 Å spectral range, while Gopka et al. (1999) determined Th at the surface of Arcturus using other lines.

A special effort was later dedicated to the observation of an increasing number of Th-rich halo stars (see for example Johnson & Bolte 2001). But the number of lines considered for the abundance determination did not necessarily increase; for example the latest investigation of Honda et al. (2004) is based on the single 4019 Å line. Numerous thorium lines were detected only in the four above-mentioned Th-rich stars.

Many authors have used the Th/Eu and other ratios to estimate the age of the observed stars, although Goriely & Clerbaux (1999) and Goriely & Arnould argued that the Th-to-Eu abundance ratio is not a reliable chronometer to derive the stellar age. New observations by Honda et al. (2004), as well as the present analysis confirm this result.

HD 221170 is one of the bright template halo stars. This seven-magnitude star has been investigated regularly as new methods and new observational facilities became available. The first paper in this series was Wallerstein et al. (1963), followed by Gilroy (1988) and many others. The last detailed abundance pattern of heavy elements in this star was provided by Burris et al. (2000). Yushchenko et al. (2002) published preliminary results for the abundances of elements heavier than Dy. However, for such elements the majority of the spectral lines are located at wavelengths shorter than 4500 Å, and the low signal-to-noise ratio obtained in this spectral region at that time required further investigations. Gopka et al. (2004, hereafter Paper I) used the spectral data from the above-mentioned work and the spectrum from the archive of the Haute-Provence Observatory 1.88 m telescope to derive the abundance of elements with $Z \leq 68$. Previous investigations concerning the surface abundances of HD 221170 and the determination of atmospheric parameters are reviewed in Paper I. According to Burris et al. (2000), Gopka et al. (2001) and Paper I, the iron abundance in HD 221170 is deficient by about 2 dex with respect to the sun while the abundance of elements heavier than barium are overabundant with respect to iron. Nevertheless, since the spectrum used in Paper I from the Haute-Provence Observatory covers the limited wavelength range of 4480–6820 Å, we were unable to determine the abundance of elements heavier than Dy.

In Sect. 2, new observations of higher quality and broader wavelength coverage are detailed and the adopted atmospheric parameters described. In Sect. 3 the result of the abundance analysis is presented. In Sect. 4, the surface abundances of HD 221170 are compared with those of the other r-process-enriched halo stars already observed, and their implication concerning the non-universality of the r-process is discussed.

2. Observations and atmospheric parameters

The observations were conducted with the Coude-echelle spectrometer (Musaev et al. 1999) mounted at the 2-m "Zeiss" telescope at the Peak Terskol observatory located near Mt. Elbrus (Northern Caucasus, Russia) 3124 m above sea level. The spectrometer is used in the mode with a spectral resolution of 45 000. The best signal-to-noise ratio is over 250 in the red spectral region and the wavelength coverage includes the 3638–10 275 Å range. Galazutdinov (1992) DECH20 and Yushchenko (1998) URAN codes are used for the data processing.

In Paper I, based on previous investigations of the star and new spectral data, the following model atmosphere parameters of HD 221170 were found to be optimum: $T_{\rm eff} = 4475 \pm 50$ K for the effective temperature, $\log\ g = 1.0 \pm 0.1$ for the gravity, $v_{\rm micro} = 1.7 \pm 0.1$ km s^{-1} for the microturbulence and $v_{\rm macro} = 4.0 \pm 0.5$ km s^{-1} for the macroturbulence.

These parameters and the abundances from Paper I are used to construct individual atmosphere models using the standard Kurucz's ATLAS12 code. We find for the final model that the correlation(s) of iron abundances with excitation potentials and equivalent widths of iron lines are close to zero.

We also calculated the models corresponding to the parameter sets ($T_{\rm eff} = 4475$ K; $\log\ g = 1.2$) and ($T_{\rm eff} = 4575$ K; $\log\ g = 1.0$). These models are used to estimate the abundance errors due to possible uncertainties in the adopted value of the temperature and gravity.

3. Abundance analysis

The equivalent widths of the iron lines are estimated by fitting their profiles with a Gaussian function. The iron abundance is calculated using the model atmosphere method on the basis of the Kurucz (1995) WIDTH9 program. In contrast, differential spectrum synthesis methods are used for all the other elements. For each line, we tried to find its counterpart in the solar spectrum atlas of Delbouille et al. (1973). This procedure frees us from uncertainties connected with oscillator strengths of spectral lines. The URAN code (Yushchenko 1998) and SYNTHE spectrum synthesis program (Kurucz 1995) are used to approximate the observed spectrum with the synthetic one. The solar abundances of Grevesse & Sauval (1999) are considered. A synthetic spectrum of HD 221170 for the whole wavelength range helps us to identify spectral lines. SYNTHE program (Kurucz 1995) was used to produce the synthetic spectrum. Atomic and molecular lines are included from Kurucz (1995) as well as Morton (2000), Biemont et al. (2002) and partially from the VALD database (Piskunov et al. 1995)

Holweger's partition function for thorium is used (Morell et al. 1992). Hyperfine structure and isotopic splitting are taken into account for Li, Sc, V, Mn, Co, Cu, Ba, and Eu. The splitting data for Li are taken from Shavrina et al. (2003), for Ba – from

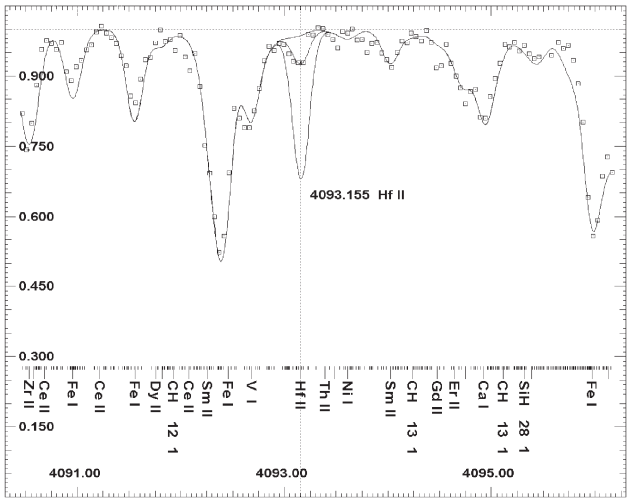

Fig. 1. The observed spectrum of HD 221170 (squares) and the synthetic spectra (solid lines) calculated with our final abundances. The axes are the wavelength in angstroms and relative fluxes. The positions of the spectral lines taken into account in the calculations are marked in the bottom part of the figure by short and long dashes. For some of the strong lines, the identification and isotopic composition for molecular lines are given. The position of the Hf II 4093.155 Å line is marked by a vertical dotted line. The different synthetic spectra correspond to a Hf abundance lower or higher by 0.5 dex with respect to the abundance obtained from the optimum value.

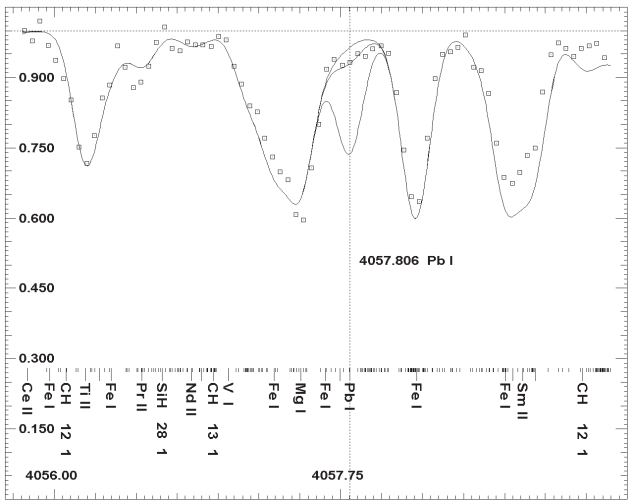

Fig. 2. Same as Fig. 1 in the vicinity of the Pb I 4057.806 Å line. The three different synthetic spectra correspond to the optimum lead abundance and a deviation by ±0.5 dex from this value. Note that the unmarked strong line on the blueside of the Pb line corresponds to the ^{12}CH line. The separation of the ^{12}CH and Pb lines is smaller than the instrumental profile, so that the uncertainties in the determination of the wavelength and oscillator strength can strongly affect the Pb abundance determination.

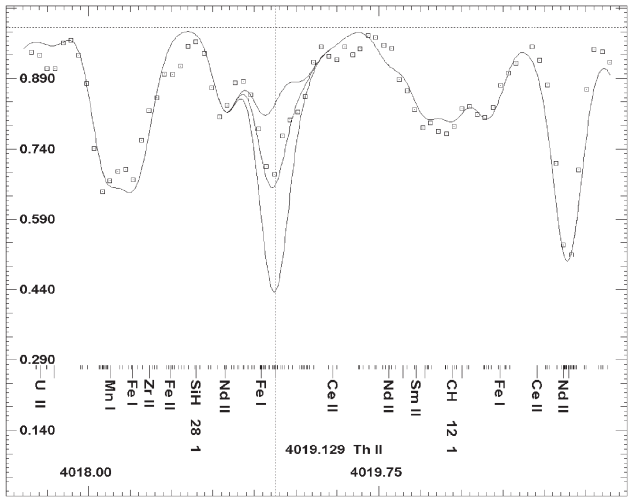

Fig. 3. Same as Fig. 1 in the vicinity of the Th II 4019.129 Å line. The different synthetic spectra correspond to the mean thorium abundance of −1.18 (in the scale log N(H) = 12) and a deviation by ±0.5 dex from this value.

Francois (1996) and for other elements from Kurucz (1995). We found counterparts in the solar spectrum for all elements except Li, S, K, Ir, Th, and U, so that the differential abundances are not strongly influenced by splitting effects.

This is true if the lines have approximately the same strength in both stars. However, HD 221170 and the Sun are different stars and it is quite difficult to find lines of similar intensity. For example, for Hf the equivalent widths of two of lines used are of the order of 2 and 3.5 mÅ in the Sun and near 45 and 15 mÅ in HD 221170. The first line, λ 3918.094 Å, with an equivalent width of 2 and 45 mÅ in the spectra of the Sun and HD 221170, respectively, shows a relative abundance difference of hafnium −0.97 dex in the atmosphere of HD 221170 with respect to the solar atmosphere. In the case of the second line, λ 4093.155 Å, the difference in the equivalent width is smaller (3.5 and 15 mÅ) and the relative abundance is −1.49 dex. We can expect that taking into account the splitting of the lines will decrease the overabundance of Hf with respect to iron in the atmosphere of HD 221170. The value obtained using the second line is therefore expected to be more reliable. But even this value shows a non-negligible deviation with respect to the solar r-process pattern, as will be shown in the next section of this paper.

For the lines of several heavy elements (U, Th, Os, Ir), no counterparts in the solar spectrum exist, and therefore the latest values of the oscillator strength (Nilsson et al. 2002a,b; Ivarsson 2003) are adopted. Several lines of hafnium, lead, thorium and uranium can be found in Figs. 1–6. The line data of iron and other chemical elements observed in the photosphere of HD 221170 are available in Tables 1 and 2, at the websites: "`users.odessa.net/~yua`" and "`yushchenko.netfirms.com`" as well as in the electronic version of the Journal at EDP.

Tables 1 and 2 contain data on lines for iron and other chemical elements. Table 1 provides the ionization stage, equivalent width, oscillator strength, energy of lower level and derived iron abundance for each iron wavelength considered. For the other elements, Table 2 gives in addition to the line data (identification, wavelength, oscillator strength, the energy of lower level), the abundance determination (relative abundance with respect to the solar system value, and absolute values of the abundance calculated from this line using the spectrum of HD 221170 and the solar spectrum), the levels of

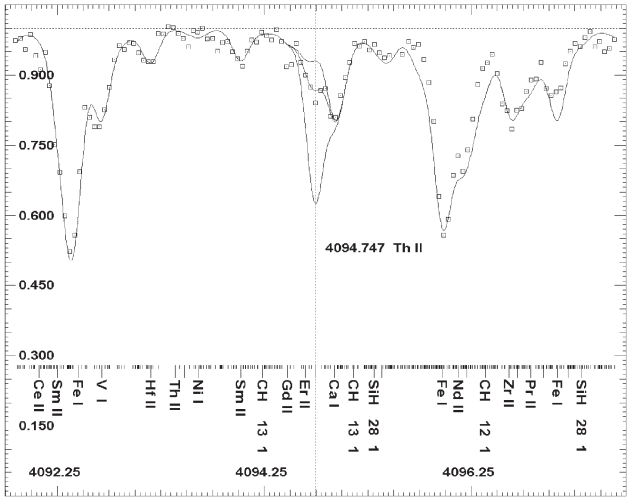

Fig. 4. Same as Fig. 3 in the vicinity of the Th II 4094.747 Å line.

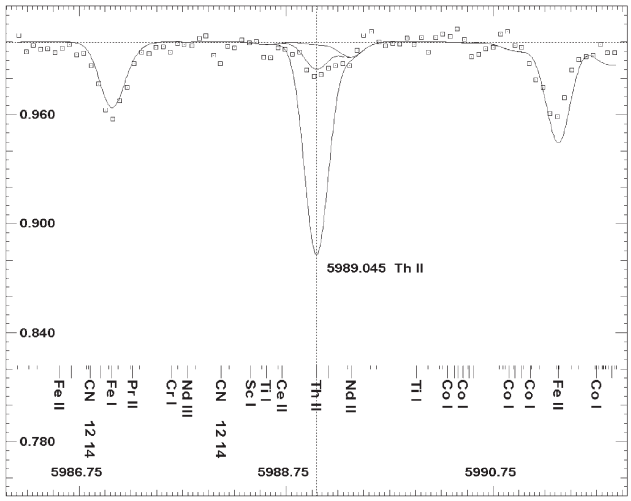

Fig. 5. Same as Fig. 3 in the vicinity of the Th II 5989.045 Å line.

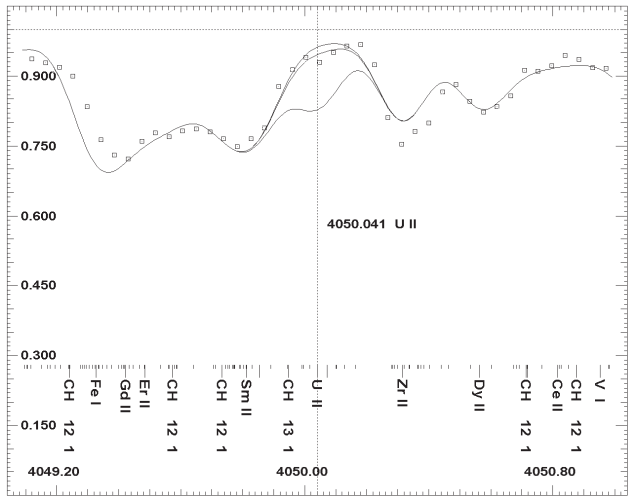

Fig. 6. Same as Fig. 1 in the vicinity of the U II 4050.041 Å line. The different synthetic spectra correspond to a uranium abundance of −2.52, −2.02, and −1.72 (in the scale log N(H) = 12).

blending of the line in the synthetic spectra of HD 221170 and of the Sun, the depths of the line in the synthetic spectra of HD 221170 and of the Sun, and the abundances in the atmosphere of HD 221170, calculated with two different atmosphere models, namely for a surface gravity increased by 0.2 dex, and for an effective temperature increased by 100 K.

In Table 3, the mean elemental abundances in the atmosphere of HD 221170 are given with respect to the solar atmosphere value. For all investigated elements, Table 3 includes information on the atomic number, designation of the ionization stage, as well as the relative abundances (the last digits in brackets correspond to the estimated errors) and the number of lines determined in Paper I and in the present study. Mean abundances are calculated with the best set of atmosphere parameters, with a surface gravity increased by 0.2 dex and with an effective temperature increased by 100 K. The absolute abundances are available in the electronic version of the table. A comparison of our abundances with previously published data can be found in Paper I. The abundances of S and Pb can be found here for the first time. The abundances of Mo, Er, Tm, Hf, W, Os, Ir, Th, and U first determined by Yushchenko et al. (2002) are updated in the present study.

In Table 4 we show the differential and absolute abundances of iron and some of the key elements used to trace back the nucleosynthesis and corresponding cosmochronometry discussed below. The errors correspond to the standard deviations of abundances derived from the individual lines of the element. For uranium and thorium, only lines with new oscillator strengths are considered.

Concerning the detection of carbon and nitrogen, their atomic lines are hardly detectable, so that their abundance determinations are usually based on molecular lines. We calculated several synthetic spectra in the whole observed region using different C and O abundances and found abundances close to −2.7 and −2.13 with respect to the Sun. This result is in good agreement with Sneden et al. (1986) and Craft et al. (1992), so that it is adopted in the abundance determination of the other elements. Special attention was also paid to the determination of the isotopic carbon ratio which can strongly influence the final results. To estimate the $^{12}C/^{13}C$ ratio, several synthetic spectra were calculated and compared with observation. We finally obtained the value of $^{12}C/^{13}C = 6$ in agreement with the determination of Sneden et al. (1986).

The wavelengths of several ^{13}CH lines were changed according to Johnson & Bolte (2001). The corresponding list of spectral lines in the vicinity of the Th II 4019.128 Å line was considered in our calculations. Note that our result concerning the thorium abundance is based on 5 lines with Nilsson et al. (2002) oscillator strengths. Similar abundances are obtained with all these lines. We therefore recommend them for future abundance determinations in other stars.

4. Discussion

About half of the stable nuclei heavier than iron in the Universe are synthesized by the rapid neutron-capture process, also

Table 3. The mean abundances of chemical elements in the atmosphere of HD 221170 with respect to their abundances in the solar atmosphere.

			Paper I				This paper			
			Haute-Provence		Terskol		Terskol, new spectrum			
	Z	Ident.	$[N/N_{\rm H}]$	n	$[N/N_H]$	n	$[N/N_{\rm H}]$			n
			ATLAS9		ATLAS9		ATLAS12	log g+0.2	$T_{\rm eff}$+100 K	
1	3	Li I					<−1.64(20)	<−1.64(20)	<−1.64(20)	2
2	6	C[1]					−2.7			
3	7	N[1]					−2.13			
4	8	O I	−1.86	1			−1.70(07)	−1.66(08)	−1.68(12)	5
5	11	Na I	−2.43(00)	2	−2.22(05)	2	−2.50(09)	−2.51(08)	−2.43(11)	3
6	12	Mg I	−1.69(08)	2	−1.89(05)	2	−1.76(09)	−1.77(09)	−1.64(12)	4
7	13	Al I	<−1.73	2			<−2.11(02)	<−1.99(09)	<−1.95(05)	2
8	14	Si I	−1.63(08)	6	−1.60(05)	3	−1.77(16)	−1.76(17)	−1.71(17)	26
		Si II					−1.75	−1.73	−1.78	1
9	16	S I					−1.72	−1.64	−1.85	1
10	19	K I					−1.55(11)	−1.57(11)	−1.34(14)	2
11	20	Ca I	−1.86(07)	21	−1.84(15)	10	−1.96(12)	−1.98(12)	−1.86(11)	31
		Ca II					−1.67(03)	−1.58(03)	−1.78(03)	2
12	21	Sc I					−1.96(09)	−1.97(08)	−1.81(17)	3
		Sc II	−1.93(08)	9	−1.92(00)	2	−2.12(13)	−2.06(13)	−2.08(11)	20
13	22	Ti I	−2.00(09)	43	−1.97(07)	8	−2.00(12)	−2.01(09)	−1.81(09)	84
		Ti II	−1.77(10)	19	−1.86(14)	9	−1.76(07)	−1.80(11)	−1.86(10)	42
14	23	V I	−2.20(09)	11	−2.10	1	−2.27(13)	−2.22(11)	−1.98(11)	34
		V II					−2.22(12)	−2.22(17)	−2.23(18)	6
15	24	Cr I	−2.26(09)	10	−2.20(01)	2	−2.23(09)	−2.32(11)	−2.10(16)	32
		Cr II	−2.03(12)	3	−2.12(14)	3	−2.02(08)	−2.08(18)	−2.04(10)	10
16	25	Mn I	−2.57(08)	8	−2.81	1	−2.37(13)	−2.42(09)	−2.25(08)	12
17	26	Fe I	−2.03(11)	187	−2.04(16)	58	−2.09(07)	−2.10(07)	−1.92(10)	221
		Fe II	−2.04(11)	23	−1.99(07)	5	−2.09(17)	−2.02(17)	−2.12(17)	30
18	27	Co I	−1.76(11)	8	−1.77(11)	3	−2.05(12)	−2.08(12)	−1.88(13)	22
19	28	Ni I	−2.07(08)	50	−2.12(11)	15	−2.07(08)	−2.13(08)	−1.99(07)	80
20	29	Cu I	−2.87(05)	2	−2.88(01)	2	−2.82	−2.82	−2.64	1
21	30	Zn I	−1.83	1			−1.82(03)	−1.87(04)	−1.90(04)	2
22	38	Sr I	−2.23	1	−2.02	1	−2.33	−2.31	−2.12	1
		Sr II			−2.15	1	−2.22	−2.26	−2.36	1
23	39	Y II	−2.12(10)	10	−2.22(15)	5	−2.10(04)	−2.12(05)	−2.15(05)	13
24	40	Zr I	−2.23	1	−2.12	1	−2.04(09)	−1.94(01)	−1.81(10)	2
		Zr II			−2.01	1	−2.09(16)	−2.13(21)	−2.14(18)	4
25	42	Mo I			−2.22	1	−2.47	−2.47	−2.34	1
26	56	Ba II	−1.86(04)	2	−2.10	1	−2.09(12)	−2.52(21)	−2.52(20)	3
27	57	La II	−1.89(05)	6	−1.94(03)	3	−1.90(06)	−1.88(09)	−1.90(12)	12
28	58	Ce II	−1.93(12)	13	−1.95(15)	14	−1.92(09)	−1.90(10)	−1.91(09)	33
29	59	Pr II	−1.51(13)	5	−1.56(08)	3	−1.56(14)	−1.53(14)	−1.55(15)	11
30	60	Nd II	−1.60(08)	25	−1.62(11)	12	−1.67(10)	−1.64(09)	−1.66(09)	51
31	62	Sm II	−1.54(11)	6	−1.64(05)	3	−1.59(08)	−1.56(06)	−1.58(06)	12
32	63	Eu II	−1.58	1	−1.57(09)	2	−1.54(13)	−1.46(18)	−1.47(20)	6
33	64	Gd II			−1.55(09)	3	−1.60(10)	−1.57(12)	−1.60(12)	5
34	66	Dy II	−1.55	1	−1.25(11)	6	−1.34(15)	−1.34(12)	−1.38(10)	7
35	68	Er II	−1.35	1	−1.38	1	−1.41(04)	−1.36(06)	−1.37(04)	2
36	69	Tm II					−1.15	−1.23	−1.24	1
37	72	Hf II					−1.23(26)	−1.12(15)	−1.14(14)	2
38	74	W I					−1.69(17)	−1.80(19)	−1.62(01)	2
39	76	Os I					−1.23(13)	−1.33(13)	−1.14(13)	4
40	77	Ir I					−1.18	−1.12	−1.10	1
41	82	Pb I					−1.85	−1.87	−1.60	1
42	90	Th II					−1.21(12)	−1.18(15)	−1.19(14)	7
		Th II[2]					−1.27(11)	−1.23(13)	−1.23(14)	5
43	92	U II					<−1.45(30)	<−1.45(30)	<−1.45(30)	8
		U II[2]					<−1.55(19)	<−1.55(19)	<−1.55(19)	5

[1] Adopted from molecular lines.
[2] Only lines with Nilsson et al. (2002a,b) oscillator strengths.

Table 4. Abundance of iron and of some elements determined in the present work. The columns provide, respectively, the atomic number, the element symbol, the number of lines analyzed, the mean abundance in the atmosphere of HD 221170 with respect to solar photosphere (Grevesse & Sauval 1998) and the abundance in the scale log N(H) = 12.

Z	Ident.	N	$\Delta\log N$	$\log N$
26	Fe I	221	–2.09+0.07	5.41 ± 0.07
	Fe II	30	–2.09+0.17	5.41 ± 0.17
63	Eu II	6	–1.54+0.13	–1.03 ± 0.13
76	Os I	4	–1.23+0.12	0.22 ± 0.12
77	Ir I	1		0.17 ± 0.20
82	Pb I	1	–1.85+0.20	0.10 ± 0.20
90	Th II	5		–1.18 ± 0.11
92	U II	5		<–2.02 ± 0.20

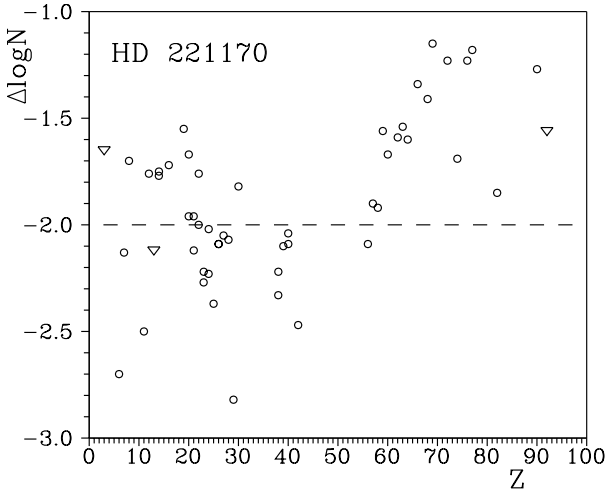

Fig. 7. The abundances of chemical elements and ions in the atmosphere of HD 221170 with respect to the solar atmosphere value. Triangles correspond to upper limits for Li, Al, U.

known as the r-process. The r-process is believed to occur predominantly in the latest stages of evolution of massive stars (heavier than about 10 solar masses) during their supernova explosion. Figure 8 compares HD 221170 abundances with the solar content in r-process nuclei. It clearly shows that for elements heavier than Ba (Z = 56), the HD 221170 surface abundance pattern is very similar to the solar one. Globally, it confirms the previous observation of ultra-metal-poor stars (Westin et al. 2000; Cayrel et al. 2001; Hill et al. 2002; Cowan et al. 2002; Sneden et al. 1998, 2003) that already in the early age of the Galaxy, the r-process was operational and quite unique in its production of, at least, the Z = 56 to 78 elements all along the life of the Galaxy. However, the universality of the r-process for the production of elements Z > 56, including the Pb-peak elements and the actinides, still remains to be confirmed. Such a universality has deep implications including in particular the invariance of the relative r-nuclidic abundances with respect to galactic chemical evolution effects and the possibility to

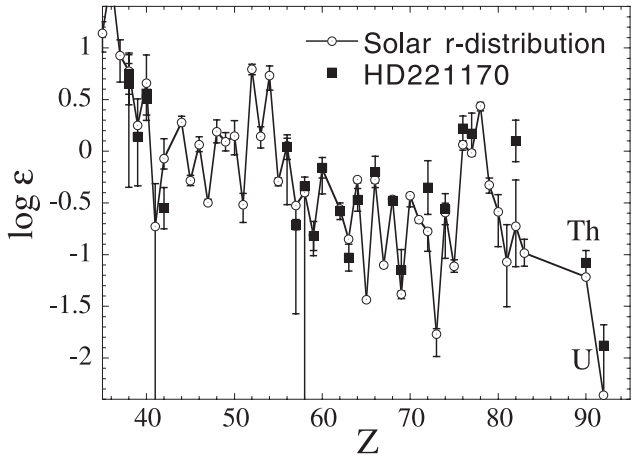

Fig. 8. Comparison of the surface abundances in HD 221170 with the solar system r-abundance distribution scaled to the observed Er abundance. The solar system abundances corresponds to the photospheric determination of Grevesse & Sauval (1998) with the solar r-process distribution estimated by Goriely (1999).

develop a stellar chronometry based on the actinide content of the metal-poor stars and consequently to estimate a lower limit to the age of the Galaxy.

Although for most of the elements with Z = 56–78 the present observations seem to comfirm this conclusion, the specific cases of Eu and Hf observed in HD 221170 show the first indication of a non-negligible deviation with respect to the solar pattern (Fig. 8). Such a deviation remains rather small, but, as shown by Goriely & Arnould (1997), large deviations are not expected in this mass region because of the nuclear correlations inherent to the nuclear aspects of the r-process nucleosynthesis. It was shown in the previous section that taking into account the hyperfine and isotopic structure of Hf lines could reduce the deviation but not to the extent to become compatible with the solar pattern. In the case of Eu, the abundance determination includes the splitting effects in both HD 221170 and the Sun.

In this comparison with the solar r-abundance distribution, another interesting feature of HD 221170 is its high Pb surface abundance. Such an unusually high abundance has been already observed in the previous ultra-metal-poor r-process-enriched stars except CS31082-001. Lead can be efficiently produced by the r-process, but also by the slow neutron-capture process, known as the s-process, during the AGB phase of low-metallicity stars with masses in the range 0.8–8 solar masses (Van Eck et al. 2001). Such a Pb s-enrichment is however systematically accompanied by a simultaneous carbon enrichment. For this reason, the significant Pb enrichment of a star like CS22892-052 characterized by a large C/O > 1 ratio could be explained by additional C and Pb s-process enrichment from a companion star. But, in the specific case of HD 221170, its low C/O = 0.025 ratio characteristic of heavy mass stars tend to argue against this possibility. The high Pb content of HD 221170 provides the second strong hint that the r-process might not be universal in its production of the elements above Ba.

Table 5. Comparison of abundance ratios (in log scale) in Th-rich stars. The second column gives the metallicity in terms of [Fe/H].

Star	[Fe/H]	Th/Eu	Th/Pb	Th/U
HD 221170	–2.1	–0.15	–1.28	>0.84
CS31082-001[a]	–2.9	–0.22	>–0.78	0.94
CS22892-052[b]	–3.1	–0.62	–1.62	>0.73
HD 115444[c]	–3.0	–0.60	–1.8[d]	>0.40
BD+17°3248[e]	–2.1	–0.51	>–1.48	>0.82

[a] Hill et al. (2002).
[b] Sneden et al. (2003).
[c] Westin et al. (2000) for all ratios except Th/Pb.
[d] Th: Westin et al. (2000), Pb: Sneden et al. (1998).
[e] Cowan et al. (2002).

Finally, the present observation provides an accurate determination of the surface Th as well as an upper limit of U abundances in HD 221170. These actinides have been used extensively in recent years to estimate the age of the oldest metal-poor stars of the Galaxy and in so doing, a lower limit to the age of our Galaxy. The Th/Eu, Th/Pb and Th/U abundance ratios in HD 221170 are compared in Table 5 to the corresponding ratios determined in the other four r-process-rich metal-poor stars. These ratios are of particular interest since they compare the Th abundance to light species (represented here by Eu), Pb (believed to be produced in the same "environment" as Th, see e.g. Goriely & Clerbaux 1999) and U, a neighboring element. Based on the universality of the r-process, a relatively reliable Th/U chronometry can be built. An absolute determination of the Th and U abundances has been achieved for CS31082-001 only, leading to an age estimate of 13 ± 4 Gyr (Hill et al. 2002; Goriely & Arnould 2001). From Table 5, it can be deduced from the Th/U ratio that, within the universality assumption, HD 221170 is older or at most 2 Gyr younger than CS31082-001.

The HD 221170 Th/Eu ratio is seen to be the highest among the different stars, which is compatible with its relatively higher metallicity [Fe/H]. However, assuming the universality of the r-process, i.e. the same original actinide production in all these stars (relative to the $Z = 56-78$ r-elements), this would imply that HD 221170 is younger than CS22892-052 by about 22 ± 4 Gyr, but also younger by 17 ± 4 Gyr than BD+17°3248, a star of similar metallicity. This would imply that BD+17°3248 would be at least 28 Gyr old, an observation that is difficult to reconcile with the traditional Big-Bang cosmology or the WMAP observation It is also seen that as far as the Th/Eu ratio is concerned, HD 221170 is compatible with CS31082-001, clearly confirming that the Th-rich star CS31082-001 is not a rare exceptional case. This conclusion was also drawn by Honda et al. (2004) who determined at the surface of CS30306-132 a ratio of [Th/Eu] = −0.10 even higher than for CS31082-001 or HD 221170. The Th/Pb ratios shown in Table 5 again confirms the previous conclusion that there is a large scatter in the r-abundances for the heaviest elements. The Th/Pb chronometry assuming the universality of the r-process would lead to the conclusion that HD 115444 is older than CS31082-001 (of similar metallicity) by about 48 ± 14 Gyr.

5. Conclusion

We determined the abundances of 43 chemical elements (including Th and U) in the atmosphere of the bright halo star HD 221170. The present spectroscopic observation indicates that the r-process is not universal or more exactly the astrophysical site(s) hosting the r-process do(es) not always lead to a unique relative abundance distribution for the bulk Ba to Hg elements, the Pb-peak elements, and the actinides. Although the previous observations of CS22892-052, HD 115444 and BD+17°3248 suggested the universal feature of the r-process, the present HD 221170 analysis confirms the non-universal trend originally suggested by the CS31082-001 observation. This new finding rules out the use of thorium chronometry to estimate the age of the oldest stars in the Galaxy.

Acknowledgements. We would like to thank to L. Delbouille and G. Roland for sending us the Liege Solar Atlas. We use data from NASA ADS, SIMBAD, CADC, VALD, NIST, and DREAM databases and we thank the teams and administrations of these projects. Work by A.Y. and Y.K. was supported by the Astrophysical Research Center for the Structure and Evolution of the Cosmos (ARCSEC) of Korea Science and Engineering Foundation (KOSEF) through the Science Research Center (SRC) program. Work by V.G. and C.K. was supported by research funds of Chonbuk National University, Korea. S.G. is FNRS Research Associate.

References

Biemont, J., Palmeri, P., & Quinet, P. 2002, Database of rare earths at Mons University
http://www.umh.ac.be/ästro/dream.html
Burris, D., Pilachowski, C. A., Armandroff, T. E., et al. 2000, ApJ, 544, 302
Cayrel, R., Hill, V., Beers, T. C., et al. 2001, Nature, 409, 691
Cowan, J. J., Sneden, C., Burles, S., et al. 2002, ApJ, 572, 861
Delbouille, L., Roland, G., & Neven, L. 1973, Photometric Atlas of the Solar Spectrum from λ3000 to λ10000, Liége: Institut d'Astrophysique de l'Université de Liege
Francois, P., Spite, M., & Spite, F. 1993, A&A, 274, 821
Galazutdinov, G. A. 1992, SAO RAS Preprint No. 92
Gilroy, K. K., Sneden, C., Pilachowski, C., & Cowan, J. 1988, ApJ, 327, 298
Gopka, V. F., Yushchenko, A. V., Shavrina, A. V., & Perekhod, A. V. 1999, Kinematika Fiz. Nebesn. Tel., 15, 447
Gopka, V., Yushchenko, A., Mishenina, T., & Kovtyukh, V. L. 2001, Odessa Astron. Publ., 14, 237
Gopka, V. F., Yushchenko, A. V., Mishenina, T. V., et al. 2004, Astron. Rep., 48, 577 (Paper I)
Goriely, S., & Arnould, M. 1997, A&A, 322, L29
Goriely, S. 1999, A&A, 342, 881
Goriely, S., & Clerbaux, B. 1999, A&A, 346, 798
Goriely, S., & Arnould, M. 2001, A&A, 379, 1113
Grevesse, N., & Sauval, A. J. 1998, Space Sci. Rev., 85, 161
Grevesse, N., & Sauval, A. J. 1999, A&A, 347, 348

Hill, V., Plez, B., Cayrel, R., et al. 2002, A&A, 387, 560
Honda, S., Aoki, W., Kajino, T., Ando, H., et al. 2004, ApJ, 607, 474
Ivarsson, S., Andersen, J., Nordstrom, B., et al. 2003, A&A, 409, 1141
Johnson, J., & Bolte, M. 2001, ApJ, 554, 888
Kurucz, R. L. 1995, ASP Conf. Ser., 81, 583
Kraft, R. P., Sneden, C., Langer, G. E, & Prosser, C. F. 1992, AJ, 104, 645
Musaev, F., Galazutdinov, G., Sergeev, A., Karpov, N., & Pod'yachev, Y. 1999, Kinematics Phys. Select. Bodies, 15, 216
Nilsson, H., Ivarsson, S., Johansson, S., & Lundberg, H. 2002a, A&A, 381, 1090
Nilsson, H., Zhang, Z., Lundberg, H., Johansson, S., & Nordstrom, B. 2002b, A&A, 382, 368
Shavrina, A. V., Polosukhina, N. S., Pavlenko, Ya. V., et al. 2003, A&A, 409, 707
Sneden, C., Cowan, J. J., Burris, D. L., & Truran, J. W. 1998, ApJ, 496, 235
Sneden, C., Cowan, J. J., Lawler, J. E., et al. 2003, ApJ, 591, 936
Van Eck, S., Goriely, S., Jorissen, A., & Plez, B. 2001, Nature, 412, 793
Wallerstein, G., Greenstein, J. L., & Parker, R. 1963, ApJ, 137, 280
Westin, J., Sneden, C., Gustafsson, B., & Cowan, J. 2000, ApJ, 530, 783
Yushchenko, A. V. 1998, Proc. of the 29th conf. of variable star research, Brno, Czech Republic, November 5–9, 201
Yushchenko, A. V., & Gopka, V. F. 1994, Astron. Lett., 20, 453
Yushchenko, A., Gopka, V., Kim, C., et al. 2002, J. Korean Astron. Soc., 35, 209
Yushchenko, A. V., Gopka, V. F., Kim, C., et al. 2004, A&A, 413, 1105

Online Material

Table 1. Iron lines in the spectrum of HD 221170.

λ (Å)	Ident.	Eq. width (mÅ)	log gf	E_{low} (eV)	log N log N(H) = 12
4531.150	Fe I	122.0	−2.15	1.485	5.548
4547.850	Fe I	48.0	−1.01	3.546	5.478
4587.130	Fe I	12.0	−1.78	3.573	5.393
4602.000	Fe I	60.0	−3.15	1.608	5.340
4602.940	Fe I	120.0	−1.95	1.485	5.276
4619.290	Fe I	30.0	−1.12	3.602	5.280
4630.120	Fe I	56.0	−2.60	2.278	5.576
4632.910	Fe I	78.0	−2.91	1.608	5.449
4637.500	Fe I	37.0	−1.39	3.283	5.294
4638.010	Fe I	38.0	−1.12	3.602	5.444
4647.430	Fe I	70.0	−1.31	2.949	5.437
4668.130	Fe I	58.0	−1.29	3.266	5.572
4669.170	Fe I	29.0	−1.21	3.653	5.410
4678.850	Fe I	60.0	−.66	3.602	5.412
4704.950	Fe I	12.0	−1.57	3.686	5.321
4707.270	Fe I	71.0	−1.08	3.241	5.589
4741.530	Fe I	44.0	−2.00	2.831	5.458
4786.810	Fe I	45.0	−1.61	3.017	5.316
4800.650	Fe I	12.0	−1.03	4.142	5.340
4807.710	Fe I	11.0	−2.20	3.368	5.506
4872.140	Fe I	111.0	−.60	2.882	5.481
4885.430	Fe I	22.0	−1.09	3.881	5.390
4886.330	Fe I	23.0	−.74	4.154	5.401
4890.750	Fe I	123.0	−.39	2.875	5.511
4903.310	Fe I	99.0	−.93	2.882	5.541
4909.380	Fe I	15.0	−1.27	3.928	5.414
4910.020	Fe I	36.0	−1.54	3.396	5.537
4917.230	Fe I	12.0	−1.18	4.191	5.531
4918.020	Fe I	7.0	−1.36	4.230	5.504
4924.770	Fe I	78.0	−2.22	2.278	5.572
4938.810	Fe I	86.0	−1.08	2.875	5.388
4950.100	Fe I	28.0	−1.67	3.417	5.522
4967.890	Fe I	28.0	−.62	4.191	5.435
4969.920	Fe I	20.0	−.71	4.217	5.359
4983.270	Fe I	45.0	−.16	4.154	5.274
4983.870	Fe I	60.0	−.07	4.103	5.408
4985.250	Fe I	47.5	−.49	3.928	5.369
4985.550	Fe I	70.0	−1.51	2.865	5.460
4994.130	Fe I	122.0	−2.96	.915	5.406
5001.860	Fe I	70.0	−.03	3.881	5.285
5005.710	Fe I	66.0	−.18	3.883	5.355
5006.120	Fe I	111.0	−.77	2.832	5.540
5014.940	Fe I	58.0	−.25	3.943	5.343
5022.240	Fe I	44.0	−.53	3.984	5.411
5044.210	Fe I	34.0	−2.15	2.851	5.406
5048.430	Fe I	16.0	−1.26	3.959	5.467
5049.820	Fe I	117.0	−1.42	2.278	5.556
5051.630	Fe I	137.0	−2.80	.915	5.564

Table 1. continued.

λ (Å)	Ident.	Eq. width (mÅ)	log gf	E_{low} (eV)	log N log N(H) = 12
5079.220	Fe I	86.0	−2.07	2.198	5.441
5083.340	Fe I	118.0	−2.96	.958	5.347
5090.770	Fe I	29.0	−.40	4.256	5.309
5097.000	Fe I	35.0	−.28	4.283	5.348
5123.720	Fe I	120.0	−3.07	1.011	5.559
5127.360	Fe I	112.0	−3.31	.915	5.487
5137.400	Fe I	43.0	−.40	4.177	5.487
5141.740	Fe I	62.0	−2.15	2.424	5.349
5151.910	Fe I	109.0	−3.32	1.011	5.567
5162.290	Fe I	65.5	.02	4.177	5.501
5166.280	Fe I	130.0	−4.20	.000	5.473
5194.940	Fe I	122.0	−2.09	1.557	5.352
5195.470	Fe I	43.0	−.23	4.220	5.366
5196.080	Fe I	22.0	−.70	4.256	5.433
5198.710	Fe I	85.0	−2.13	2.223	5.492
5215.180	Fe I	68.0	−.93	3.266	5.320
5216.270	Fe I	120.0	−2.15	1.608	5.422
5217.390	Fe I	63.0	−1.10	3.211	5.325
5225.520	Fe I	93.0	−4.79	.110	5.439
5242.490	Fe I	46.0	−.97	3.634	5.422
5247.050	Fe I	84.0	−4.95	.087	5.405
5250.210	Fe I	83.0	−4.94	.121	5.419
5250.650	Fe I	89.0	−2.05	2.198	5.438
5253.020	Fe I	4.5	−3.94	2.278	5.392
5253.460	Fe I	32.0	−1.67	3.283	5.410
5263.310	Fe I	73.0	−.97	3.266	5.447
5281.790	Fe I	90.0	−.83	3.038	5.359
5307.360	Fe I	77.0	−2.99	1.608	5.377
5322.040	Fe I	28.0	−3.03	2.278	5.402
5364.860	Fe I	53.0	.22	4.445	5.371
5367.480	Fe I	62.0	.35	4.415	5.382
5369.960	Fe I	67.0	.35	4.371	5.414
5379.570	Fe I	17.0	−1.48	3.694	5.364
5389.480	Fe I	26.0	−.41	4.415	5.426
5391.460	Fe I	23.0	−.82	4.154	5.440
5393.170	Fe I	88.0	−.71	3.241	5.431
5398.280	Fe I	13.0	−.67	4.445	5.346
5400.500	Fe I	38.0	−.16	4.371	5.373
5403.820	Fe I	15.0	−1.03	4.076	5.318
5410.910	Fe I	54.0	.28	4.473	5.361
5415.190	Fe I	70.0	.50	4.386	5.335
5436.590	Fe I	20.0	−3.24	2.278	5.410
5445.040	Fe I	48.0	−.02	4.386	5.437
5462.950	Fe I	29.0	−.23	4.473	5.387
5466.390	Fe I	21.0	−.63	4.371	5.467
5473.900	Fe I	21.0	−.76	4.154	5.322
5483.100	Fe I	4.5	−1.58	4.154	5.386
5497.520	Fe I	134.0	−2.85	1.011	5.483

Table 1. continued.

λ (Å)	Ident.	Eq. width (mÅ)	log gf	E_{low} (eV)	log N log N(H) = 12
5501.460	Fe I	121.0	−3.05	.958	5.349
5506.780	Fe I	132.0	−2.80	.990	5.363
5522.450	Fe I	4.0	−1.55	4.209	5.370
5554.880	Fe I	20.0	−.44	4.548	5.463
5560.210	Fe I	5.5	−1.19	4.434	5.429
5565.700	Fe I	19.0	−.28	4.607	5.343
5576.090	Fe I	63.0	−1.00	3.430	5.465
5618.630	Fe I	6.5	−1.38	4.209	5.415
5624.040	Fe I	4.0	−1.48	4.386	5.517
5633.980	Fe I	9.0	−.27	4.991	5.418
5638.260	Fe I	19.0	−.87	4.220	5.452
5653.890	Fe I	2.0	−1.64	4.386	5.369
5662.520	Fe I	32.0	−.54	4.177	5.373
5686.520	Fe I	15.0	−.63	4.548	5.488
5701.540	Fe I	55.0	−2.22	2.559	5.407
5717.840	Fe I	11.0	−1.13	4.284	5.509
5752.020	Fe I	5.5	−1.00	4.548	5.373
5753.120	Fe I	21.5	−.76	4.260	5.454
5760.350	Fe I	3.0	−2.49	3.641	5.469
5775.080	Fe I	9.0	−1.20	4.220	5.396
5862.350	Fe I	25.0	−.36	4.548	5.490
5883.810	Fe I	17.0	−1.36	3.959	5.541
5916.250	Fe I	23.0	−2.99	2.453	5.422
5930.170	Fe I	26.0	−.23	4.652	5.508
5956.690	Fe I	44.0	−4.61	.859	5.358
5976.770	Fe I	15.0	−1.31	3.943	5.402
5984.810	Fe I	19.0	−.34	4.733	5.536
6003.010	Fe I	25.0	−1.12	3.881	5.410
6007.960	Fe I	9.2	−.66	4.652	5.390
6008.550	Fe I	25.0	−1.08	3.883	5.376
6012.210	Fe I	5.0	−4.04	2.223	5.429
6024.050	Fe I	36.0	−.12	4.548	5.473
6027.050	Fe I	15.0	−1.21	4.076	5.467
6055.990	Fe I	12.5	−.46	4.733	5.435
6065.480	Fe I	90.0	−1.53	2.608	5.355
6082.710	Fe I	17.0	−3.57	2.223	5.532
6136.990	Fe I	40.0	−2.95	2.198	5.371
6137.690	Fe I	105.0	−1.40	2.588	5.447
6151.620	Fe I	22.0	−3.30	2.176	5.330
6173.340	Fe I	41.0	−2.88	2.223	5.348
6180.200	Fe I	18.0	−2.78	2.727	5.412
6191.560	Fe I	109.0	−1.42	2.433	5.334
6200.310	Fe I	35.0	−2.44	2.608	5.299
6213.430	Fe I	64.0	−2.48	2.223	5.316
6219.280	Fe I	75.0	−2.43	2.198	5.412
6232.640	Fe I	30.0	−1.27	3.653	5.363
6240.650	Fe I	26.0	−3.23	2.223	5.409
6246.320	Fe I	57.0	−.96	3.602	5.478

Table 1. continued.

λ (Å)	Ident.	Eq. width (mÅ)	log gf	E_{low} (eV)	log N log N(H) = 12
6252.550	Fe I	100.0	−1.69	2.404	5.386
6265.130	Fe I	70.5	−2.55	2.176	5.421
6270.220	Fe I	20.0	−2.46	2.858	5.306
6290.970	Fe I	9.0	−.67	4.733	5.472
6297.790	Fe I	51.0	−2.74	2.223	5.360
6302.490	Fe I	28.0	−1.20	3.686	5.288
6311.500	Fe I	6.0	−3.23	2.831	5.455
6318.020	Fe I	86.0	−1.80	2.453	5.297
6322.690	Fe I	44.0	−2.43	2.588	5.411
6335.330	Fe I	84.0	−2.23	2.198	5.344
6336.820	Fe I	42.0	−1.05	3.686	5.406
6344.150	Fe I	31.0	−2.92	2.433	5.469
6355.030	Fe I	32.0	−2.37	2.845	5.467
6393.600	Fe I	105.0	−1.62	2.433	5.413
6400.000	Fe I	81.0	−.52	3.602	5.429
6408.020	Fe I	38.0	−1.05	3.686	5.327
6411.650	Fe I	62.0	−.82	3.653	5.471
6419.940	Fe I	19.0	−.24	4.733	5.411
6421.350	Fe I	91.0	−2.03	2.278	5.381
6430.840	Fe I	105.0	−2.01	2.176	5.435
6475.630	Fe I	21.5	−2.94	2.559	5.426
6481.870	Fe I	33.0	−2.98	2.278	5.351
6494.980	Fe I	132.0	−1.27	2.404	5.477
6518.370	Fe I	23.0	−2.46	2.831	5.329
6546.240	Fe I	92.0	−1.54	2.758	5.523
6575.020	Fe I	26.0	−2.82	2.588	5.444
6581.210	Fe I	10.0	−4.68	1.485	5.383
6592.910	Fe I	90.0	−1.60	2.727	5.498
6593.870	Fe I	51.0	−2.42	2.433	5.290
6609.110	Fe I	28.0	−2.69	2.559	5.315
6750.150	Fe I	48.0	−2.62	2.424	5.418
6828.590	Fe I	7.0	−.92	4.638	5.453
6839.830	Fe I	9.5	−3.42	2.559	5.471
6843.650	Fe I	8.0	−.93	4.548	5.412
6855.160	Fe I	16.0	−.49	4.558	5.326
6945.200	Fe I	49.0	−2.48	2.424	5.278
6978.850	Fe I	53.0	−2.50	2.484	5.434
7016.060	Fe I	17.0	−3.21	2.424	5.363
7022.950	Fe I	13.0	−1.25	4.191	5.510
7038.220	Fe I	10.0	−1.30	4.217	5.466
7086.720	Fe I	2.5	−2.68	3.602	5.425
7090.380	Fe I	13.5	−1.21	4.230	5.535
7130.920	Fe I	28.0	−.79	4.217	5.492
7151.470	Fe I	7.5	−3.68	2.484	5.503
7164.440	Fe I	41.0	−.53	4.191	5.448
7219.680	Fe I	6.0	−1.69	4.076	5.426
7445.750	Fe I	47.0	−.24	4.256	5.325
7461.520	Fe I	8.0	−3.55	2.559	5.478

Table 1. continued.

λ (Å)	Ident.	Eq. width (mÅ)	log gf	E_{low} (eV)	log N log N(H) = 12
7491.650	Fe I	12.0	−1.01	4.301	5.345
7511.020	Fe I	79.0	.11	4.177	5.398
7568.890	Fe I	25.0	−.68	4.283	5.377
7583.790	Fe I	47.0	−1.89	3.017	5.374
7710.360	Fe I	14.0	−1.05	4.220	5.348
7723.200	Fe I	14.0	−3.62	2.278	5.435
7748.270	Fe I	59.0	−1.76	2.949	5.329
7832.190	Fe I	52.0	.02	4.434	5.348
7912.860	Fe I	41.0	−4.85	.859	5.382
7945.840	Fe I	61.0	.12	4.386	5.324
7998.940	Fe I	52.0	−.27	4.371	5.543
8028.310	Fe I	11.0	−.94	4.473	5.413
8047.620	Fe I	50.0	−4.70	.859	5.350
8085.180	Fe I	42.0	−.24	4.445	5.435
8387.770	Fe I	152.0	−1.49	2.176	5.358
8439.560	Fe I	13.0	−.70	4.548	5.328
8468.400	Fe I	111.0	−2.07	2.223	5.388
8515.110	Fe I	53.0	−1.92	3.017	5.425
8582.260	Fe I	34.0	−2.13	2.990	5.287
8611.800	Fe I	68.0	−1.90	2.845	5.400
8621.600	Fe I	36.0	−2.32	2.949	5.460
8674.740	Fe I	81.0	−1.85	2.831	5.510
8688.620	Fe I	179.0	−1.21	2.176	5.395
8757.180	Fe I	54.0	−2.03	2.845	5.309
8838.420	Fe I	61.0	−2.05	2.858	5.440
8866.920	Fe I	44.0	−.06	4.548	5.362
8868.430	Fe I	18.0	−2.65	3.017	5.471
8999.560	Fe I	110.0	−1.30	2.831	5.366
9088.310	Fe I	85.0	−1.89	2.845	5.584
4508.290	Fe II	74.5	−2.21	2.855	5.202
4515.340	Fe II	70.0	−2.48	2.844	5.373
4520.220	Fe II	65.0	−2.60	2.806	5.325
4541.520	Fe II	54.7	−3.05	2.855	5.609
4555.890	Fe II	75.0	−2.29	2.828	5.258
4576.340	Fe II	48.0	−3.04	2.844	5.445
4582.840	Fe II	30.7	−3.10	2.844	5.142
4620.520	Fe II	30.2	−3.28	2.828	5.289
4666.760	Fe II	32.0	−3.33	2.828	5.383
4731.450	Fe II	44.1	−3.36	2.891	5.732
4993.360	Fe II	18.0	−3.65	2.806	5.293
5100.660	Fe II	8.4	−4.37	2.806	5.620
5197.580	Fe II	68.9	−2.10	3.230	5.338
5234.630	Fe II	71.1	−2.05	3.221	5.316
5256.940	Fe II	9.0	−4.25	2.891	5.620
5264.810	Fe II	23.3	−3.19	3.230	5.478
5276.000	Fe II	82.0	−1.94	3.199	5.399

Table 1. continued.

λ (Å)	Ident.	Eq. width (mÅ)	log gf	E_{low} (eV)	log N log N(H) = 12
5284.110	Fe II	40.0	−3.19	2.891	5.428
5325.550	Fe II	22.0	−2.60	3.221	4.842
5362.870	Fe II	55.0	−2.74	3.199	5.646
5414.070	Fe II	9.0	−3.79	3.221	5.555
5425.260	Fe II	19.6	−3.36	3.199	5.504
5534.850	Fe II	34.0	−2.93	3.245	5.470
5991.380	Fe II	13.0	−3.56	3.153	5.406
6084.110	Fe II	7.6	−3.81	3.199	5.446
6247.560	Fe II	27.0	−2.33	3.891	5.473
6432.680	Fe II	18.0	−3.71	2.891	5.383
6456.380	Fe II	40.0	−2.08	3.903	5.504
6516.080	Fe II	31.3	−3.45	2.891	5.441
7711.720	Fe II	14.0	−2.54	3.903	5.253

Table 2. Lines of other elements in the spectrum of HD 221170.

Code (Fe I = 26.00)	λ (Å)	log gf	E_{low} (eV)	Δlog N $*-\odot$	log N (log N(H) = 12) Star	Sun	Blending (1 = clean line) Star	Sun	Depth in synt. spectra Star	Sun	Error for log g +0.2	Error for T_{eff} +100 K
3.00	6707.761	−0.009	0.000	<−1.437	<−0.337		*hfs*		*hfs*			
3.00	6707.912	−0.309	0.000	<−1.847	<−0.747		*hfs*		*hfs*			
8.00	6300.304	−9.710	0.000	−1.662	7.146	8.808	0.974	0.785	0.166	0.041	0.071	0.048
8.00	6363.776	−10.300	0.020	−1.743	7.087		0.995		0.040		0.057	0.044
8.00	7771.944	0.320	9.146	−1.598	7.278	8.876	1.000	1.000	0.032	0.365	0.056	−0.112
8.00	7774.166	0.170	9.146	−1.818	7.011	8.829	0.986	0.998	0.014	0.328	0.015	−0.055
8.00	7775.388	−0.050	9.146	−1.688	7.117	8.805	0.564	0.998	0.011	0.279	0.014	0.193
11.00	5682.633	−0.700	2.102	−2.495	3.920	6.415	0.999	1.000	0.072	0.720	−0.006	0.072
11.00	5688.205	−0.450	2.104	−2.613	3.944	6.557	0.922	0.994	0.124	0.778	−0.006	0.047
11.00	8183.255	0.230	2.102	−2.386	3.944		1.000		0.315		−0.018	0.094
12.00	4571.096	−5.690	0.000	−1.865	5.465	7.330	1.000	1.000	0.886	0.896	−0.019	0.345
12.00	4730.029	−2.520	4.346	−1.824	5.919	7.743	0.932	1.000	0.104	0.621	0.000	−0.028
12.00	5711.088	−1.830	4.346	−1.741	5.876	7.617	1.000	1.000	0.311	0.725	−0.012	0.094
12.00	7387.689	−1.020	5.753	−1.610	5.834	7.444	0.966	0.979	0.388	0.004	−0.006	0.051
13.00	6696.023	−1.350	3.143	<−2.086	<4.132	6.218	0.891	0.941	0.015	0.310	0.001	0.085
13.00	6698.673	−1.650	3.143	<−2.128	<4.132	6.260	0.654	0.995	0.008	0.207	0.226	0.229
14.00	5517.533	−2.380	5.082	−1.830	5.653	7.483	0.823	1.000	0.012	0.162	0.284	0.222
14.00	5645.613	−2.140	4.930	−1.759	5.858	7.617	0.996	1.000	0.051	0.373	0.001	0.054
14.00	5665.555	−2.040	4.920	−1.958	5.591	7.549	0.848	0.996	0.036	0.393	0.000	0.000
14.00	5675.417	−1.030	5.619	−1.544	5.713	7.257	0.644	0.773	0.067	0.397	−0.010	0.098
14.00	5684.484	−1.650	4.954	−1.926	5.649	7.575	1.000	1.000	0.086	0.562	0.010	0.061
14.00	5690.425	−1.870	4.930	−1.786	5.801	7.587	0.955	0.975	0.080	0.488	−0.001	0.059
14.00	5701.104	−2.050	4.930	−1.588	6.008	7.596	1.000	1.000	0.085	0.405	−0.004	0.052
14.00	5708.400	−1.470	4.954	−1.966	5.651	7.617	1.000	1.000	0.125	0.634	0.000	0.145
14.00	5772.146	−1.750	5.082	−1.668	5.955	7.623	1.000	1.000	0.095	0.482	−0.011	0.058
14.00	5793.073	−2.060	4.930	−2.024	5.606	7.630	0.931	0.982	0.034	0.412	0.000	0.000
14.00	5797.856	−2.050	4.954	−1.789	5.879	7.668	0.993	1.000	0.060	0.423	−0.035	0.048
14.00	5948.541	−1.230	5.082	−1.702	5.879	7.581	1.000	1.000	0.216	0.636	0.003	0.057
14.00	6155.135	−0.400	5.619	−1.630	5.484	7.114	0.999	1.000	0.143	0.569	0.006	0.052
14.00	6237.320	−0.530	5.614	−1.568	5.382	6.950	1.000	1.000	0.091	0.467	0.008	0.059
14.00	6243.815	−0.770	5.616	−1.907	5.148	7.055	0.996	0.999	0.033	0.412	0.009	0.040
14.00	6721.848	−1.490	5.863	−1.794	6.059	7.853	0.982	0.996	0.025	0.324	−0.346	0.053
14.00	7034.901	−0.880	5.871	−2.047	5.606	7.653	0.993	0.997	0.035	0.466	0.250	0.018
14.00	7165.545	−1.520	5.871	−1.706	6.656	8.362	0.954	1.000	0.082	0.482	−0.030	0.038
14.00	7184.885	−1.690	5.614	−1.538	5.981	7.519	0.991	0.984	0.027	0.211	0.012	0.051
14.00	7250.627	−1.040	5.619	−1.797	5.692	7.489	1.000	1.000	0.056	0.437	0.009	0.047
14.00	7289.175	−0.200	5.619	−1.628	5.488	7.116	1.000	1.000	0.189	0.563	0.006	0.036
14.00	7405.772	−0.820	5.614	−1.594	6.154	7.748	0.999	0.997	0.207	0.562	0.006	0.051
14.00	7415.948	0.310	5.616	−1.689	4.889	6.578	1.000	1.000	0.163	0.554	0.009	0.043
14.00	7423.496	−0.310	5.619	−1.657	5.707	7.364	1.000	1.000	0.223	0.585	0.008	0.050
14.00	7742.717	−0.690	6.206	−2.145	5.591	7.736	0.211	0.815	0.021	0.414	0.000	0.000
14.00	7944.001	−0.310	5.984	−1.695	5.954	7.649	1.000	1.000	0.159	0.543	0.018	0.041
14.01	6347.109	0.300	8.121	−1.755	5.606	7.361	0.761	0.988	0.018	0.335	0.029	−0.021
16.00	9212.863	0.420	6.525	−1.721	5.609		0.998		0.273		0.083	−0.133
19.00	7664.911	0.130	0.000	−1.436	3.684		1.000		0.648		−0.014	0.247
19.00	7698.974	−0.170	0.000	−1.672	3.448		1.000		0.561		−0.015	0.185

Table 2. continued.

Code (Fe I = 26.00)	λ (Å)	log gf	E_{low} (eV)	Δlog N $* - \odot$	log N (log N(H) = 12) Star	log N Sun	Blending (1 = clean line) Star	Blending Sun	Depth in synt. spectra Star	Depth in synt. spectra Sun	Error for log g +0.2	Error for T_{eff} +100 K
20.00	4318.652	−0.295	1.899	−2.178	4.237	6.415	0.999	1.000	0.776	0.935	−0.035	0.150
20.00	4425.437	−0.286	1.879	−2.091	4.214	6.305	1.000	1.000	0.771	0.927	−0.047	0.149
20.00	4455.887	−0.414	1.899	−2.000	4.281	6.281	1.000	1.000	0.754	0.919	−0.040	0.136
20.00	4456.616	−1.590	1.899	−1.767	4.435	6.202	0.861	0.959	0.336	0.791	−0.006	0.042
20.00	4526.928	−0.907	2.709	−1.931	4.703	6.634	0.993	1.000	0.311	0.835	−0.008	0.098
20.00	4578.551	−0.170	2.521	−1.968	3.841	5.809	0.992	1.000	0.363	0.846	−0.015	0.098
20.00	4585.865	0.161	2.526	−1.900	3.917	5.817	1.000	1.000	0.563	0.878	−0.023	0.100
20.00	4685.268	−0.544	2.933	−1.685	4.271	5.956	0.991	1.000	0.169	0.683	−0.009	0.073
20.00	5260.387	−1.720	2.521	−1.858	4.459	6.317	0.992	1.000	0.062	0.455	−0.021	0.061
20.00	5261.704	−0.591	2.521	−1.989	4.438	6.427	1.000	1.000	0.427	0.820	−0.018	0.103
20.00	5265.556	−0.148	2.523	−2.012	4.420	6.432	1.000	1.000	0.602	0.854	−0.063	0.078
20.00	5349.465	−1.178	2.709	−1.882	5.304	7.186	1.000	1.000	0.444	0.809	−0.022	0.104
20.00	5512.980	−0.712	2.933	−1.918	4.671	6.589	1.000	1.000	0.237	0.746	−0.013	0.084
20.00	5581.965	−0.569	2.523	−2.057	4.364	6.421	1.000	1.000	0.388	0.800	−0.113	0.006
20.00	5590.114	−0.596	2.521	−1.977	4.420	6.397	1.000	1.000	0.404	0.795	−0.018	0.106
20.00	5594.462	0.051	2.523	−2.264	4.367	6.631	0.996	1.000	0.623	0.857	−0.022	0.107
20.00	5598.480	−0.134	2.521	−2.148	4.411	6.559	1.000	1.000	0.585	0.843	0.045	0.119
20.00	5601.277	−0.552	2.526	−1.932	4.456	6.388	0.997	1.000	0.438	0.796	−0.018	0.106
20.00	5857.451	0.257	2.933	−2.012	4.367	6.379	1.000	1.000	0.508	0.809	−0.022	0.104
20.00	6102.723	−0.862	1.879	−1.906	4.605	6.511	1.000	1.000	0.636	0.812	−0.019	0.161
20.00	6161.297	−1.293	2.523	−1.987	4.404	6.391	0.995	0.999	0.122	0.627	−0.024	0.101
20.00	6166.439	−1.156	2.521	−1.929	4.474	6.403	1.000	1.000	0.181	0.668	0.000	0.100
20.00	6169.042	−0.804	2.523	−1.913	4.532	6.445	1.000	1.000	0.341	0.738	−0.021	0.100
20.00	6169.563	−0.527	2.526	−1.972	4.517	6.489	1.000	1.000	0.450	0.774	−0.022	0.105
20.00	6449.808	−1.015	2.521	−2.081	4.924	7.005	1.000	1.000	0.410	0.760	−0.021	0.114
20.00	6455.598	−1.557	2.523	−1.724	4.844	6.568	1.000	1.000	0.167	0.587	−0.016	0.096
20.00	6471.662	−0.653	2.526	−1.926	4.480	6.406	1.000	1.000	0.373	0.734	−0.006	0.082
20.00	6499.650	−0.719	2.523	−1.855	4.438	6.293	1.000	1.000	0.329	0.707	−0.029	0.094
20.00	6572.779	−4.104	0.000	−2.066	4.084	6.150	0.993	0.974	0.139	0.400	−0.020	0.187
20.00	6717.681	−0.596	2.709	−1.815	4.611	6.426	1.000	1.000	0.348	0.704	−0.019	0.104
20.00	7202.200	−0.807	2.709	−1.999	5.060	7.059	0.998	1.000	0.428	0.725	−0.020	0.121
20.01	8912.068	0.575	7.047	−1.636	5.110	6.746	1.000	1.000	0.190	0.500	0.092	−0.103
20.01	8927.356	−0.572	7.050	−1.707	5.211	6.918	0.985	0.997	0.246	0.546	0.086	−0.109
21.00	4047.794	−3.001	0.021	−2.074	1.211	3.285	*hfs*	*hfs*	*hfs*	*hfs*	0.003	0.009
21.00	5671.822	−0.238	1.448	−1.835	1.013	2.848	*hfs*	*hfs*	*hfs*	*hfs*	−0.027	0.153
21.00	6305.662	−2.625	0.021	−1.971	0.840	2.811	*hfs*	*hfs*	*hfs*	*hfs*	−0.011	0.281
21.01	4246.820	−0.876	0.315	−2.264	0.294	2.558	*hfs*	*hfs*	*hfs*	*hfs*	0.047	0.090
21.01	4294.767	−1.945	0.606	−2.015	1.001	3.016	*hfs*	*hfs*	*hfs*	*hfs*	0.055	0.051
21.01	4305.714	−1.846	0.595	−2.216	0.607	2.823	*hfs*	*hfs*	*hfs*	*hfs*	0.041	0.170
21.01	4314.084	−1.166	0.618	−2.363	0.542	2.905	*hfs*	*hfs*	*hfs*	*hfs*	0.026	0.085
21.01	4320.733	−1.511	0.605	−2.345	0.580	2.925	*hfs*	*hfs*	*hfs*	*hfs*	0.056	0.066
21.01	4354.597	−2.626	0.605	−2.105	0.974	3.079	*hfs*	*hfs*	*hfs*	*hfs*	0.046	0.040
21.01	4400.389	−1.175	0.606	−2.402	0.627	3.029	*hfs*	*hfs*	*hfs*	*hfs*	0.067	0.080
21.01	4431.353	−3.131	0.605	−2.027	0.990	3.017	*hfs*	*hfs*	*hfs*	*hfs*	0.072	0.049
21.01	4670.406	−1.621	1.357	−2.014	0.888	2.902	*hfs*	*hfs*	*hfs*	*hfs*	0.050	−0.007
21.01	5031.025	−1.272	1.357	−2.127	0.802	2.929	*hfs*	*hfs*	*hfs*	*hfs*	0.066	0.018
21.01	5239.813	−0.770	1.455	−1.952	1.181	3.133	*hfs*	*hfs*	*hfs*	*hfs*	0.079	0.021
21.01	5318.358	−2.563	1.357	−2.031	1.236	3.267	*hfs*	*hfs*	*hfs*	*hfs*	0.048	0.030
21.01	5526.801	−0.523	1.768	−2.185	0.864	3.049	*hfs*	*hfs*	*hfs*	*hfs*	0.085	0.021
21.01	5552.214	−2.650	1.455	−1.983	1.284	3.267	*hfs*	*hfs*	*hfs*	*hfs*	0.015	0.018
21.01	5640.991	−1.563	1.500	−2.045	1.118	3.163	*hfs*	*hfs*	*hfs*	*hfs*	0.066	0.012

Table 2. continued.

Code (Fe I = 26.00)	λ (Å)	log gf	E_{low} (eV)	Δlog N $* - \odot$	log N (log N(H) = 12) Star	log N Sun	Blending (1 = clean line) Star	Blending Sun	Depth in synt. spectra Star	Depth in synt. spectra Sun	Error for log g +0.2	Error for T_{eff} +100 K
21.01	5657.896	−1.126	1.507	−2.074	1.023	3.097	*hfs*	*hfs*	*hfs*	*hfs*	0.079	0.016
21.01	5667.149	−1.834	1.500	−2.005	1.178	3.183	*hfs*	*hfs*	*hfs*	*hfs*	0.076	0.018
21.01	5669.053	−1.500	1.500	−1.999	1.178	3.177	*hfs*	*hfs*	*hfs*	*hfs*	0.042	0.006
21.01	5684.195	−2.062	1.507	−2.059	1.104	3.163	*hfs*	*hfs*	*hfs*	*hfs*	0.074	0.017
21.01	6604.601	−2.106	1.357	−2.112	1.275	3.387	*hfs*	*hfs*	*hfs*	*hfs*	0.069	0.009
22.00	3900.958	−1.691	0.021	−1.925	3.070	4.995	0.993	0.998	0.611	0.817	−0.012	0.234
22.00	3998.636	−0.056	0.048	−2.127	2.408	4.535	1.000	1.000	0.895	0.953	−0.032	0.288
22.00	4008.926	−1.072	0.021	−2.258	2.704	4.962	0.996	1.000	0.743	0.930	−0.034	0.224
22.00	4060.263	−0.520	1.053	−2.122	2.596	4.718	0.993	0.999	0.239	0.729	−0.018	0.169
22.00	4112.708	−1.758	0.048	−2.064	2.910	4.974	0.991	0.995	0.441	0.749	−0.002	0.148
22.00	4263.134	0.260	1.887	−1.985	2.485	4.470	0.562	0.681	0.112	0.533	−0.050	0.026
22.00	4295.751	−0.450	0.813	−1.977	2.850	4.827	0.994	0.994	0.696	0.870	−0.083	0.179
22.00	4417.273	−0.020	1.887	−2.037	2.714	4.751	0.700	0.915	0.126	0.531	0.007	0.289
22.00	4449.143	0.500	1.887	−1.925	2.874	4.799	0.989	0.997	0.417	0.812	−0.060	0.105
22.00	4450.896	0.410	1.879	−1.911	2.855	4.766	0.971	0.994	0.360	0.776	−0.068	0.082
22.00	4453.315	−0.051	1.430	−1.870	3.051	4.921	0.972	0.980	0.546	0.824	−0.057	0.135
22.00	4453.708	−0.010	1.873	−1.846	3.149	4.995	0.986	0.998	0.300	0.693	−0.042	0.129
22.00	4455.321	0.000	1.443	−1.766	2.899	4.665	0.939	0.885	0.476	0.749	−0.081	0.162
22.00	4457.428	0.180	1.460	−1.780	3.000	4.780	0.907	0.983	0.623	0.837	−0.089	0.055
22.00	4512.733	−0.480	0.836	−2.007	2.946	4.953	1.000	1.000	0.706	0.865	−0.065	0.154
22.00	4518.023	−0.325	0.826	−2.014	2.887	4.901	1.000	1.000	0.759	0.879	−0.071	0.153
22.00	4527.305	−0.470	0.813	−1.842	2.994	4.836	0.995	1.000	0.750	0.852	−0.127	0.012
22.00	4534.778	0.280	0.836	−1.992	2.797	4.789	1.000	1.000	0.901	0.913	−0.184	0.070
22.00	4535.570	0.120	0.826	−2.117	2.710	4.827	1.000	1.000	0.845	0.907	−0.127	0.123
22.00	4544.688	−0.520	0.818	−2.001	3.000	5.001	1.000	1.000	0.726	0.867	−0.009	0.213
22.00	4548.765	−0.354	0.826	−1.989	2.940	4.929	1.000	1.000	0.764	0.878	−0.079	0.153
22.00	4555.485	−0.488	0.848	−1.968	2.973	4.941	0.999	1.000	0.706	0.858	−0.046	0.168
22.00	4617.254	0.389	1.749	−2.041	2.842	4.883	0.976	1.000	0.435	0.826	−0.035	0.134
22.00	4623.094	0.110	1.739	−2.036	2.848	4.884	0.968	0.992	0.293	0.750	−0.034	0.152
22.00	4639.358	−0.021	1.739	−1.858	3.000	4.858	1.000	0.997	0.298	0.676	−0.027	0.100
22.00	4656.468	−1.345	0.000	−2.301	2.685	4.986	1.000	1.000	0.841	0.870	0.116	0.391
22.00	4681.908	−1.071	0.048	−2.109	2.752	4.861	1.000	1.000	0.934	0.880	0.076	0.360
22.00	4693.663	−2.710	0.021	−2.123	2.940	5.063	1.000	0.895	0.158	0.222	0.066	0.106
22.00	4715.301	−2.680	0.048	−2.015	3.000	5.015	0.941	0.957	0.179	0.203	0.040	0.052
22.00	4742.792	0.210	2.236	−1.984	2.904	4.888	1.000	1.000	0.116	0.535	−0.020	0.129
22.00	4758.120	0.425	2.249	−1.998	2.931	4.929	1.000	1.000	0.185	0.666	−0.038	0.124
22.00	4759.272	0.514	2.256	−2.047	2.879	4.926	0.995	1.000	0.197	0.704	−0.048	0.130
22.00	4840.874	−0.509	0.900	−1.998	2.848	4.846	0.991	0.992	0.582	0.807	−0.037	0.188
22.00	4885.082	0.358	1.887	−1.855	3.040	4.895	1.000	1.000	0.418	0.768	−0.055	0.124
22.00	4913.616	0.160	1.873	−1.865	3.036	4.901	1.000	1.000	0.322	0.703	−0.042	0.105
22.00	4919.867	−0.120	2.160	−1.898	3.049	4.947	0.923	0.955	0.098	0.408	0.015	0.027
22.00	4981.732	0.504	0.848	−1.848	2.979	4.827	1.000	1.000	0.968	0.901	−0.212	0.082
22.00	4991.067	0.380	0.836	−1.890	2.818	4.708	1.000	1.000	0.924	0.888	−0.167	0.098
22.00	4997.098	−2.118	0.000	−2.227	2.762	4.989	1.000	1.000	0.379	0.538	0.166	0.416
22.00	4999.504	0.250	0.826	−1.843	2.830	4.673	1.000	1.000	0.901	0.878	−0.152	0.096
22.00	5001.009	−0.034	1.997	−1.964	2.944	4.908	0.948	0.975	0.143	0.529	0.032	0.120
22.00	5009.646	−2.259	0.021	−2.216	2.785	5.001	1.000	0.999	0.289	0.438	0.146	0.387
22.00	5016.162	−0.574	0.848	−1.953	2.994	4.947	1.000	1.000	0.664	0.814	−0.054	0.172
22.00	5020.028	−0.414	0.836	−1.890	3.024	4.914	1.000	1.000	0.756	0.837	−0.078	0.153
22.00	5022.871	−0.434	0.826	−1.853	3.055	4.908	0.997	0.999	0.770	0.834	−0.091	0.145
22.00	5024.842	−0.602	0.818	−1.935	3.018	4.953	1.000	1.000	0.685	0.816	−0.054	0.178
22.00	5025.563	0.073	2.041	−1.816	3.259	5.075	0.972	0.983	0.282	0.658	−0.044	0.136
22.00	5036.468	0.130	1.443	−1.865	2.994	4.859	0.998	1.000	0.588	0.806	−0.089	0.088

Table 2. continued.

Code (Fe I = 26.00)	λ (Å)	log gf	E_{low} (eV)	Δlog N $* - \odot$	log N (log N(H) = 12) Star	log N Sun	Blending (1 = clean line) Star	Blending Sun	Depth in synt. spectra Star	Depth in synt. spectra Sun	Error for log g +0.2	Error for T_{eff} +100 K
22.00	5038.399	0.013	1.430	−1.929	2.982	4.911	1.000	1.000	0.523	0.795	−0.063	0.137
22.00	5039.959	−1.130	0.021	−2.203	2.674	4.877	1.000	1.000	0.912	0.856	0.118	0.402
22.00	5040.615	−1.787	0.826	−2.078	2.979	5.057	1.000	0.983	0.097	0.271	0.003	0.255
22.00	5043.588	−1.733	0.836	−2.177	2.856	5.033	0.980	0.970	0.082	0.281	0.052	0.208
22.00	5064.654	−0.991	0.048	−2.172	2.668	4.840	1.000	1.000	0.934	0.862	0.101	0.390
22.00	5087.055	−0.780	1.430	−1.910	2.958	4.868	0.967	0.986	0.143	0.392	−0.027	0.136
22.00	5113.448	−0.783	1.443	−2.112	2.856	4.968	0.999	1.000	0.112	0.443	−0.028	0.144
22.00	5145.464	−0.574	1.460	−1.959	3.000	4.959	1.000	0.989	0.211	0.556	−0.015	0.176
22.00	5147.479	−2.012	0.000	−2.242	2.762	5.004	0.996	1.000	0.453	0.612	0.160	0.415
22.00	5152.185	−2.024	0.021	−2.227	2.774	5.001	1.000	1.000	0.428	0.589	0.141	0.385
22.00	5210.386	−0.884	0.048	−2.230	2.552	4.782	1.000	1.000	0.935	0.857	0.089	0.406
22.00	5219.700	−2.292	0.021	−2.254	2.773	5.027	1.000	1.000	0.272	0.431	0.167	0.414
22.00	5282.380	−1.300	1.053	−2.206	2.609	4.815	0.997	0.990	0.066	0.280	0.019	0.230
22.00	5295.780	−1.633	1.067	−1.960	3.064	5.024	1.000	1.000	0.082	0.215	0.039	0.243
22.00	5426.237	−3.006	0.021	−2.122	2.932	5.054	1.000	0.986	0.088	0.120	0.195	0.452
22.00	5490.150	−0.933	1.460	−1.840	3.161	5.001	1.000	0.997	0.143	0.356	−0.004	0.191
22.00	5512.529	−0.350	1.460	−2.072	2.838	4.910	1.000	0.999	0.236	0.635	−0.025	0.178
22.00	5866.452	−0.840	1.067	−1.977	2.976	4.953	1.000	1.000	0.319	0.598	0.000	0.204
22.00	5899.297	−1.154	1.053	−1.961	3.046	5.007	1.000	0.999	0.213	0.461	0.000	0.227
22.00	5918.539	−1.460	1.067	−1.962	2.858	4.820	1.000	0.999	0.080	0.202	0.020	0.224
22.00	5922.110	−1.466	1.046	−2.151	2.862	5.013	1.000	1.000	0.083	0.291	0.019	0.235
22.00	5937.811	−1.890	1.067	−1.916	3.061	4.977	1.000	1.000	0.047	0.116	0.027	0.033
22.00	5941.752	−1.510	1.053	−1.934	2.943	4.877	0.984	0.918	0.089	0.209	0.012	0.231
22.00	5953.162	−0.329	1.887	−1.782	3.186	4.968	1.000	1.000	0.168	0.424	−0.014	0.160
22.00	5978.543	−0.496	1.873	−1.880	3.082	4.962	0.998	1.000	0.102	0.342	−0.018	0.172
22.00	6126.217	−1.425	1.067	−2.057	2.994	5.051	1.000	0.998	0.111	0.323	0.000	0.201
22.00	6258.104	−0.355	1.443	−1.941	3.018	4.959	1.000	1.000	0.323	0.627	−0.024	0.169
22.00	6258.709	−0.240	1.460	−1.917	3.024	4.941	0.977	1.000	0.372	0.654	−0.030	0.154
22.00	6261.101	−0.479	1.430	−1.856	3.097	4.953	1.000	1.000	0.311	0.576	−0.033	0.171
22.00	6743.124	−1.630	0.900	−1.993	2.918	4.911	1.000	0.988	0.101	0.235	0.028	0.258
22.00	7244.856	−0.810	1.443	−2.022	2.955	4.977	0.830	0.748	0.128	0.393	−0.017	0.207
22.00	7357.726	−1.122	1.443	−2.153	2.901	5.054	1.000	0.996	0.059	0.277	−0.017	0.181
22.00	8412.285	−1.483	0.818	−1.859	3.142	5.001	1.000	0.992	0.263	0.379	0.044	0.270
22.00	8426.497	−1.253	0.826	−1.976	3.034	5.010	1.000	0.999	0.315	0.486	0.024	0.245
22.00	8434.887	−0.781	0.848	−1.982	2.862	4.844	1.000	1.000	0.449	0.581	0.021	0.262
22.00	8435.623	−1.023	0.836	−1.995	2.958	4.953	1.000	1.000	0.383	0.546	0.036	0.265
22.01	4028.343	−1.000	1.892	−1.741	3.142	4.883	0.999	1.000	0.822	0.893	−0.188	−0.222
22.01	4290.219	−1.120	1.165	−1.814	3.145	4.959	1.000	1.000	0.905	0.933	−0.366	−0.344
22.01	4316.799	−1.420	2.048	−1.731	2.976	4.707	1.000	1.000	0.642	0.701	−0.036	−0.095
22.01	4330.695	−2.040	1.180	−1.890	2.997	4.887	1.000	0.994	0.783	0.833	−0.033	−0.051
22.01	4344.288	−2.090	1.084	−1.753	3.248	5.001	0.997	0.999	0.827	0.861	−0.304	−0.336
22.01	4394.051	−1.590	1.221	−1.655	3.085	4.740	1.000	1.000	0.840	0.869	−0.265	−0.280
22.01	4395.850	−2.170	1.243	−1.721	3.448	5.169	1.000	1.000	0.810	0.842	−0.222	−0.269
22.01	4411.925	−2.406	1.224	−1.938	2.973	4.911	1.000	0.998	0.664	0.708	−0.033	−0.103
22.01	4421.938	−1.770	2.061	−1.806	3.141	4.947	0.974	0.953	0.546	0.638	0.068	0.040
22.01	4444.558	−2.030	1.116	−1.692	3.055	4.747	1.000	1.000	0.799	0.810	−0.061	−0.201
22.01	4518.327	−2.555	1.080	−1.747	3.212	4.959	1.000	0.999	0.743	0.719	−0.113	−0.139
22.01	4524.687	−2.989	1.231	−1.875	3.082	4.957	1.000	0.991	0.411	0.389	0.045	−0.006
22.01	4568.314	−2.650	1.224	−1.745	3.000	4.745	1.000	1.000	0.562	0.469	0.006	−0.024
22.01	4583.409	−2.720	1.165	−1.726	3.112	4.838	1.000	1.000	0.616	0.516	−0.018	−0.054
22.01	4609.264	−3.260	1.180	−1.761	3.076	4.837	1.000	0.983	0.298	0.214	0.054	0.006
22.01	4636.320	−2.855	1.165	−1.716	2.911	4.627	1.000	0.990	0.434	0.312	0.034	−0.012
22.01	4655.773	−3.014	1.161	−1.749	2.813	4.562	1.000	0.815	0.302	0.209	0.050	0.005

Table 2. continued.

Code (Fe I = 26.00)	λ (Å)	log gf	E_{low} (eV)	Δlog N $*-\odot$	log N (log N(H) = 12) Star	log N Sun	Blending (1 = clean line) Star	Blending Sun	Depth in synt. spectra Star	Depth in synt. spectra Sun	Error for log g +0.2	Error for T_{eff} +100 K
22.01	4708.665	−2.210	1.237	−1.770	3.046	4.816	1.000	1.000	0.725	0.722	−0.088	−0.133
22.01	4762.776	−2.710	1.084	−1.733	3.006	4.739	1.000	1.000	0.610	0.500	−0.006	−0.006
22.01	4764.526	−2.770	1.237	−1.897	3.098	4.995	1.000	0.991	0.533	0.532	0.104	−0.022
22.01	4779.985	−1.370	2.048	−1.695	3.294	4.989	0.994	0.987	0.718	0.766	−0.104	−0.145
22.01	4798.521	−2.430	1.080	−1.812	2.902	4.714	1.000	0.998	0.679	0.647	−0.028	−0.073
22.01	4805.085	−1.100	2.061	−1.883	3.174	5.057	1.000	1.000	0.739	0.821	−0.128	−0.180
22.01	4911.193	−0.340	3.124	−1.746	2.866	4.612	0.995	0.999	0.437	0.625	0.013	−0.074
22.01	4996.367	−2.915	1.582	−1.785	3.034	4.819	1.000	0.976	0.204	0.189	0.012	−0.046
22.01	5005.157	−2.550	1.566	−1.773	3.000	4.773	1.000	0.989	0.369	0.340	0.034	−0.034
22.01	5013.677	−1.935	1.582	−1.721	2.981	4.702	1.000	0.994	0.639	0.625	−0.052	−0.083
22.01	5129.152	−1.390	1.892	−1.605	3.410	5.015	1.000	1.000	0.744	0.775	−0.216	−0.252
22.01	5154.070	−1.920	1.566	−1.748	3.306	5.054	0.998	0.999	0.717	0.744	−0.144	−0.159
22.01	5185.913	−1.350	1.893	−1.626	3.239	4.865	1.000	1.000	0.721	0.749	−0.172	−0.224
22.01	5211.536	−1.356	2.590	−1.827	2.994	4.821	0.996	1.000	0.319	0.472	0.012	−0.030
22.01	5336.771	−1.700	1.582	−1.725	3.314	5.039	1.000	1.000	0.736	0.769	−0.199	−0.256
22.01	5381.015	−2.080	1.566	−1.740	3.305	5.045	0.995	1.000	0.673	0.682	−0.074	−0.130
22.01	5396.226	−2.925	1.584	−1.843	2.946	4.789	1.000	0.963	0.171	0.169	0.060	0.012
22.01	5418.751	−1.999	1.582	−1.606	3.229	4.835	1.000	1.000	0.665	0.629	−0.090	−0.147
22.01	5490.690	−2.650	1.566	−1.706	3.142	4.848	1.000	0.991	0.380	0.315	0.050	0.007
22.01	5492.862	−2.956	1.582	−1.731	3.034	4.765	0.999	0.967	0.190	0.152	0.063	0.012
22.01	6219.940	−2.819	2.061	−1.716	2.921	4.637	1.000	0.933	0.056	0.058	0.079	0.010
22.01	6491.561	−1.793	2.061	−1.765	2.979	4.744	1.000	1.000	0.380	0.420	0.030	−0.048
22.01	6559.588	−2.019	2.048	−1.627	3.121	4.748	1.000	0.878	0.352	0.324	0.034	−0.057
22.01	6606.949	−2.790	2.061	−1.823	3.085	4.908	0.997	0.983	0.086	0.107	0.148	0.058
22.01	6680.133	−1.855	3.095	−1.852	2.886	4.738	0.674	0.690	0.025	0.071	0.090	−0.034
23.00	4092.682	−0.238	0.287	−2.117	1.457	3.574	*hfs*	*hfs*	*hfs*	*hfs*	0.026	0.245
23.00	4111.774	0.408	0.301	−2.188	1.122	3.310	*hfs*	*hfs*	*hfs*	*hfs*	0.090	0.281
23.00	4115.177	−2.016	1.955	−2.232	1.178	3.410	*hfs*	*hfs*	*hfs*	*hfs*	0.017	0.266
23.00	4116.468	−0.310	0.275	−2.353	1.034	3.387	*hfs*	*hfs*	*hfs*	*hfs*	0.056	0.303
23.00	4128.076	−0.104	0.275	−1.933	1.491	3.424	*hfs*	*hfs*	*hfs*	*hfs*	−0.065	0.204
23.00	4330.026	−2.248	0.000	−2.219	1.432	3.651	*hfs*	*hfs*	*hfs*	*hfs*	0.025	0.342
23.00	4379.230	0.580	0.301	−2.045	1.164	3.209	*hfs*	*hfs*	*hfs*	*hfs*	0.020	0.267
23.00	4384.712	0.510	0.287	−2.095	1.090	3.185	*hfs*	*hfs*	*hfs*	*hfs*	0.022	0.304
23.00	4389.976	0.200	0.275	−2.187	1.247	3.434	*hfs*	*hfs*	*hfs*	*hfs*	0.035	0.286
23.00	4406.633	−0.190	0.301	−2.311	1.217	3.528	*hfs*	*hfs*	*hfs*	*hfs*	0.064	0.303
23.00	4416.469	−1.596	0.267	−2.191	1.333	3.524	*hfs*	*hfs*	*hfs*	*hfs*	−0.036	0.258
23.00	4421.557	−0.770	0.275	−2.285	1.180	3.465	*hfs*	*hfs*	*hfs*	*hfs*	0.020	0.317
23.00	4436.133	−0.900	0.262	−2.244	1.369	3.613	*hfs*	*hfs*	*hfs*	*hfs*	0.063	0.287
23.00	4437.834	−0.660	0.287	−2.402	1.070	3.472	*hfs*	*hfs*	*hfs*	*hfs*	0.057	0.305
23.00	4459.748	−0.500	0.287	−2.127	1.317	3.444	*hfs*	*hfs*	*hfs*	*hfs*	0.060	0.286
23.00	4577.175	−1.832	0.000	−2.467	1.141	3.608	*hfs*	*hfs*	*hfs*	*hfs*	0.027	0.286
23.00	4586.374	−0.790	0.040	−2.307	1.249	3.556	*hfs*	*hfs*	*hfs*	*hfs*	0.114	0.372
23.00	4594.125	−1.549	0.069	−2.333	1.156	3.489	*hfs*	*hfs*	*hfs*	*hfs*	0.101	0.354
23.00	4619.780	−1.800	0.040	−2.415	1.235	3.650	*hfs*	*hfs*	*hfs*	*hfs*	0.115	0.353
23.00	4831.646	−1.380	0.017	−2.330	1.197	3.527	*hfs*	*hfs*	*hfs*	*hfs*	0.118	0.367
23.00	4851.483	−1.925	0.000	−2.465	1.059	3.524	*hfs*	*hfs*	*hfs*	*hfs*	0.109	0.376
23.00	4864.731	−0.960	0.017	−2.431	1.169	3.600	*hfs*	*hfs*	*hfs*	*hfs*	0.120	0.360
23.00	4875.493	−0.810	0.040	−2.242	1.329	3.571	*hfs*	*hfs*	*hfs*	*hfs*	0.106	0.364
23.00	5627.634	−1.744	1.081	−2.190	1.477	3.667	*hfs*	*hfs*	*hfs*	*hfs*	−0.050	0.149
23.00	5670.854	−1.315	1.081	−2.401	1.170	3.571	*hfs*	*hfs*	*hfs*	*hfs*	0.018	0.217
23.00	5698.520	−0.111	1.064	−2.172	1.369	3.541	*hfs*	*hfs*	*hfs*	*hfs*	0.009	0.170
23.00	5703.575	−0.779	1.051	−2.204	1.415	3.619	*hfs*	*hfs*	*hfs*	*hfs*	−0.024	0.182
23.00	5727.049	−0.907	1.081	−2.465	1.393	3.858	*hfs*	*hfs*	*hfs*	*hfs*	−0.017	0.207

Table 2. continued.

Code (Fe I = 26.00)	λ (Å)	log gf	E_{low} (eV)	Δlog N $*-\odot$	log N (log N(H) = 12) Star	log N Sun	Blending (1 = clean line) Star	Blending Sun	Depth in synt. spectra Star	Depth in synt. spectra Sun	Error for log g +0.2	Error for T_{eff} +100 K
23.00	6090.214	−0.062	1.081	−2.131	1.506	3.637	*hfs*	*hfs*	*hfs*	*hfs*	0.002	0.214
23.00	6119.523	−0.320	1.064	−2.165	1.774	3.939	*hfs*	*hfs*	*hfs*	*hfs*	0.000	0.207
23.00	6199.197	−1.300	0.287	−2.371	1.074	3.445	*hfs*	*hfs*	*hfs*	*hfs*	0.093	0.337
23.00	6216.354	−1.290	0.275	−2.367	1.271	3.638	*hfs*	*hfs*	*hfs*	*hfs*	0.090	0.357
23.00	6243.105	−0.980	0.301	−2.459	1.147	3.606	*hfs*	*hfs*	*hfs*	*hfs*	0.086	0.330
23.00	6251.827	−1.340	0.287	−2.167	1.403	3.570	*hfs*	*hfs*	*hfs*	*hfs*	0.094	0.377
23.01	3916.410	−1.060	1.428	−2.473	1.896	4.369	0.999	1.000	0.735	0.906	−0.119	−0.137
23.01	3951.965	−0.740	1.476	−2.125	1.838	3.963	0.998	1.000	0.780	0.886	−0.064	−0.122
23.01	3997.120	−1.200	1.476	−2.166	1.833	3.999	1.000	1.000	0.627	0.794	0.026	−0.020
23.01	4036.782	−1.540	1.476	−2.188	1.740	3.928	0.993	0.979	0.384	0.585	0.064	0.001
23.01	4209.759	−1.936	1.675	−2.277	1.911	4.188	0.885	0.877	0.167	0.373	0.045	0.146
23.01	4564.589	−1.450	2.268	−2.099	2.121	4.220	1.000	0.992	0.149	0.344	0.045	0.089
24.00	3849.536	−1.820	0.983	−2.141	3.263	5.404	0.859	0.983	0.463	0.852	−0.027	0.155
24.00	3852.214	−1.810	0.968	−2.126	3.205	5.331	0.975	0.975	0.445	0.835	−0.049	0.185
24.00	3908.756	−1.000	1.004	−2.396	3.030	5.426	0.994	1.000	0.766	0.945	−0.072	0.081
24.00	4351.054	−1.449	0.968	−2.196	3.204	5.400	0.954	0.998	0.652	0.892	−0.135	0.141
24.00	4540.488	−0.487	2.544	−2.265	3.356	5.621	0.847	1.000	0.174	0.789	0.006	0.080
24.00	4545.945	−1.370	0.941	−2.371	3.239	5.610	1.000	1.000	0.716	0.905	−0.104	0.127
24.00	4591.389	−1.740	0.968	−2.279	3.354	5.633	0.999	1.000	0.569	0.869	−0.051	0.154
24.00	4600.741	−1.260	1.004	−2.292	3.272	5.564	1.000	1.000	0.737	0.901	−0.121	0.100
24.00	4616.120	−1.190	0.983	−2.314	3.238	5.552	1.000	1.000	0.760	0.904	−0.131	0.095
24.00	4626.174	−1.320	0.968	−2.406	3.161	5.567	1.000	1.000	0.686	0.898	−0.086	0.157
24.00	4646.148	−0.700	1.030	−2.119	3.292	5.411	1.000	1.000	0.866	0.917	−0.268	−0.016
24.00	4651.282	−1.460	0.983	−2.364	3.233	5.597	1.000	1.000	0.642	0.888	−0.078	0.151
24.00	4652.152	−1.030	1.004	−2.253	3.227	5.480	1.000	1.000	0.791	0.906	−0.167	0.064
24.00	4697.042	−1.060	2.708	−2.062	3.684	5.746	1.000	0.997	0.069	0.482	−0.288	0.073
24.00	4708.018	0.110	3.168	−2.228	3.384	5.612	0.988	1.000	0.127	0.758	0.000	−0.009
24.00	4730.704	−0.192	3.079	−2.182	3.430	5.612	0.998	1.000	0.096	0.685	−0.006	0.024
24.00	4954.807	−0.300	3.122	−2.216	3.548	5.764	0.988	1.000	0.084	0.669	0.073	0.209
24.00	4964.916	−2.527	0.941	−2.293	3.435	5.728	1.000	1.000	0.202	0.633	−0.045	0.196
24.00	5072.917	−2.734	0.941	−2.222	3.466	5.688	0.944	0.992	0.145	0.481	−0.036	0.211
24.00	5206.038	0.019	0.941	−2.338	3.103	5.441	1.000	1.000	0.978	0.920	−0.330	0.002
24.00	5247.566	−1.640	0.961	−2.222	3.381	5.603	1.000	1.000	0.627	0.836	−0.069	0.165
24.00	5296.691	−1.400	0.983	−2.153	3.399	5.552	1.000	1.000	0.718	0.849	−0.125	0.115
24.00	5297.376	0.167	2.900	−2.062	3.526	5.588	1.000	1.000	0.321	0.783	−0.039	0.102
24.00	5298.277	−1.150	0.983	−2.239	3.245	5.484	1.000	1.000	0.748	0.863	−0.168	0.100
24.00	5300.744	−2.120	0.983	−2.303	3.366	5.669	1.000	1.000	0.337	0.755	−0.018	0.195
24.00	5329.142	−0.064	2.914	−2.243	3.396	5.639	0.895	1.000	0.168	0.742	−0.012	0.103
24.00	5345.801	−0.980	1.004	−2.096	3.378	5.474	1.000	1.000	0.815	0.869	−0.237	0.006
24.00	5348.312	−1.290	1.004	−2.198	3.330	5.528	1.000	1.000	0.716	0.851	−0.131	0.106
24.00	5409.772	−0.720	1.030	−2.105	3.330	5.435	1.000	1.000	0.853	0.876	−0.224	0.054
24.00	6330.093	−2.920	0.941	−2.313	3.436	5.749	1.000	1.000	0.095	0.384	−0.012	0.000
24.00	6979.799	−0.410	3.464	−2.245	3.534	5.779	0.268	0.990	0.023	0.366	−0.008	0.846
24.00	7400.226	−0.111	2.900	−2.109	3.548	5.657	1.000	1.000	0.190	0.625	−0.034	0.110
24.01	4558.650	−0.660	4.073	−2.176	3.602	5.778	0.998	1.000	0.509	0.816	−0.133	−0.112
24.01	4588.199	−0.630	4.071	−1.967	3.620	5.587	1.000	0.999	0.529	0.791	−0.018	−0.104
24.01	4592.049	−1.220	4.074	−1.886	3.635	5.521	1.000	1.000	0.267	0.631	0.052	−0.027
24.01	4616.629	−1.290	4.072	−2.070	3.473	5.543	0.999	0.999	0.181	0.611	−0.007	−0.025
24.01	4634.070	−1.240	4.072	−1.915	3.885	5.800	1.000	0.999	0.367	0.707	−0.399	−0.101
24.01	4824.127	−1.220	3.871	−2.131	3.737	5.868	0.873	0.996	0.416	0.754	−0.241	0.061
24.01	4848.235	−1.140	3.864	−2.006	3.533	5.539	0.974	1.000	0.361	0.699	0.000	−0.061

Table 2. continued.

Code (Fe I = 26.00)	λ (Å)	log gf	E_{low} (eV)	Δlog N $*-\odot$	log N (log N(H) = 12) Star	log N Sun	Blending (1 = clean line) Star	Blending Sun	Depth in synt. spectra Star	Depth in synt. spectra Sun	Error for log g +0.2	Error for T_{eff} +100 K
24.01	5237.329	−1.160	4.073	−2.081	3.493	5.574	0.990	0.000	0.217	0.000	−0.008	0.136
24.01	5313.563	−1.650	4.074	−1.944	3.742	5.686	1.000	1.000	0.140	0.463	0.079	−0.016
24.01	5334.869	−1.562	4.072	−2.018	3.504	5.522	0.947	0.990	0.105	0.435	0.077	0.031
25.00	4018.111	−1.015	2.114	−2.257	2.843	5.100	*hfs*	*hfs*	*hfs*	*hfs*	−0.045	0.101
25.00	4082.938	−1.081	2.178	−2.236	3.096	5.332	*hfs*	*hfs*	*hfs*	*hfs*	−0.103	0.085
25.00	4754.043	−0.951	2.282	−2.301	2.876	5.177	*hfs*	*hfs*	*hfs*	*hfs*	−0.076	0.089
25.00	4761.507	−0.564	2.953	−2.373	2.834	5.207	*hfs*	*hfs*	*hfs*	*hfs*	−0.028	0.123
25.00	4762.361	−2.688	2.888	−2.266	2.731	4.997	*hfs*	*hfs*	*hfs*	*hfs*	−0.043	0.115
25.00	4766.417	−2.602	2.920	−2.306	2.915	5.221	*hfs*	*hfs*	*hfs*	*hfs*	−0.033	0.117
25.00	4783.424	−0.738	2.298	−2.335	2.849	5.184	*hfs*	*hfs*	*hfs*	*hfs*	−0.073	0.003
25.00	4823.523	−0.562	2.319	−2.228	2.922	5.150	*hfs*	*hfs*	*hfs*	*hfs*	−0.155	0.030
25.00	5420.374	−2.169	2.143	−2.515	2.942	5.457	*hfs*	*hfs*	*hfs*	*hfs*	0.000	0.201
25.00	5432.538	−4.640	0.000	−2.677	2.646	5.323	*hfs*	*hfs*	*hfs*	*hfs*	0.013	0.299
25.00	5470.649	−2.547	2.164	−2.470	2.987	5.457	*hfs*	*hfs*	*hfs*	*hfs*	0.004	0.179
25.00	6013.478	−0.766	3.072	−2.481	2.824	5.305	*hfs*	*hfs*	*hfs*	*hfs*	−0.006	0.121
27.00	4019.299	−4.552	0.629	−1.986	3.174	5.160	*hfs*	*hfs*	*hfs*	*hfs*	−0.043	0.200
27.00	4066.369	−3.244	0.923	−2.031	2.640	4.671	*hfs*	*hfs*	*hfs*	*hfs*	−0.087	0.240
27.00	4068.540	−2.034	1.956	−1.997	3.005	5.002	*hfs*	*hfs*	*hfs*	*hfs*	−0.039	0.129
27.00	4727.933	−4.044	0.432	−2.061	2.705	4.766	*hfs*	*hfs*	*hfs*	*hfs*	−0.022	0.237
27.00	4792.846	−0.067	3.252	−2.271	2.600	4.871	*hfs*	*hfs*	*hfs*	*hfs*	−0.011	0.126
27.00	4813.467	0.050	3.216	−2.169	2.693	4.862	*hfs*	*hfs*	*hfs*	*hfs*	−0.016	0.127
27.00	4867.872	0.226	3.117	−1.812	3.062	4.874	*hfs*	*hfs*	*hfs*	*hfs*	−0.046	0.072
27.00	5230.190	−2.743	1.740	−2.270	2.788	5.058	*hfs*	*hfs*	*hfs*	*hfs*	−0.046	0.160
27.00	5247.899	−2.700	1.785	−2.034	2.908	4.942	*hfs*	*hfs*	*hfs*	*hfs*	−0.033	0.190
27.00	5301.044	−3.345	1.710	−2.034	2.825	4.859	*hfs*	*hfs*	*hfs*	*hfs*	−0.009	0.186
27.00	5342.701	−0.181	4.021	−2.105	2.963	5.068	*hfs*	*hfs*	*hfs*	*hfs*	0.003	0.117
27.00	5369.590	−2.433	1.740	−2.214	2.907	5.121	*hfs*	*hfs*	*hfs*	*hfs*	−0.020	0.179
27.00	5483.341	−2.425	1.710	−1.884	2.924	4.808	*hfs*	*hfs*	*hfs*	*hfs*	−0.033	0.174
27.00	5530.771	−2.995	1.710	−1.965	2.780	4.745	*hfs*	*hfs*	*hfs*	*hfs*	−0.011	0.165
27.00	5590.708	−2.773	2.042	−1.973	2.948	4.921	*hfs*	*hfs*	*hfs*	*hfs*	0.002	0.198
27.00	5647.235	−2.343	2.280	−2.098	2.803	4.901	*hfs*	*hfs*	*hfs*	*hfs*	0.025	0.175
27.00	6093.125	−3.343	1.740	−2.098	2.959	5.057	*hfs*	*hfs*	*hfs*	*hfs*	−0.014	0.175
27.00	6093.125	−3.343	1.740	−1.818	2.959	4.777	*hfs*	*hfs*	*hfs*	*hfs*	−0.014	0.175
27.00	6450.250	−2.633	1.710	−2.162	2.825	4.987	*hfs*	*hfs*	*hfs*	*hfs*	−0.012	0.190
27.00	6814.942	−2.922	1.956	−2.170	2.665	4.835	*hfs*	*hfs*	*hfs*	*hfs*	−0.030	0.168
27.00	7052.871	−2.223	1.956	−1.924	2.753	4.677	*hfs*	*hfs*	*hfs*	*hfs*	−0.023	0.175
27.00	7084.989	−1.648	1.883	−2.083	2.580	4.663	*hfs*	*hfs*	*hfs*	*hfs*	−0.026	0.184
28.00	3792.330	−3.240	0.275	−2.086	3.959	6.045	0.999	1.000	0.896	0.948	−0.304	−0.043
28.00	3912.971	−3.702	0.025	−1.980	3.819	5.799	0.999	1.000	0.856	0.894	−0.210	0.068
28.00	4331.640	−2.100	1.676	−2.125	3.958	6.083	0.996	1.000	0.677	0.885	−0.060	0.096
28.00	4401.538	0.080	3.193	−1.935	4.155	6.090	1.000	1.000	0.763	0.914	−0.190	0.006
28.00	4470.472	−0.400	3.399	−2.005	4.270	6.275	1.000	1.000	0.572	0.873	−0.082	0.038
28.00	4600.355	−0.610	3.597	−2.267	3.984	6.251	1.000	1.000	0.197	0.799	−0.018	0.071
28.00	4604.982	−0.290	3.480	−2.194	4.057	6.251	1.000	1.000	0.459	0.861	−0.057	0.107
28.00	4648.646	−0.160	3.420	−2.070	4.134	6.204	1.000	1.000	0.597	0.874	−0.101	0.030
28.00	4686.207	−0.640	3.597	−2.225	4.020	6.245	1.000	1.000	0.198	0.784	−0.016	0.096
28.00	4703.803	−0.735	3.658	−2.102	4.227	6.329	0.999	0.999	0.216	0.765	−0.017	0.093
28.00	4714.408	0.230	3.380	−1.932	4.176	6.108	1.000	1.000	0.728	0.892	−0.227	−0.084
28.00	4715.757	−0.340	3.543	−2.085	4.128	6.213	1.000	1.000	0.428	0.837	−0.061	0.048
28.00	4756.510	−0.340	3.480	−2.178	4.047	6.225	0.995	1.000	0.427	0.844	−0.029	0.099
28.00	4806.984	−0.640	3.679	−2.161	4.079	6.240	0.993	1.000	0.186	0.753	−0.017	0.097

Table 2. continued.

Code (Fe I = 26.00)	λ (Å)	log gf	E_{low} (eV)	Δlog N $*-\odot$	log N (log N(H) = 12) Star	log N Sun	Blending (1 = clean line) Star	Blending Sun	Depth in synt. spectra Star	Depth in synt. spectra Sun	Error for log g +0.2	Error for T_{eff} +100 K
28.00	4829.016	−0.330	3.542	−1.993	4.210	6.203	1.000	1.000	0.473	0.827	−0.046	0.054
28.00	4852.547	−1.070	3.542	−2.114	4.179	6.293	0.976	0.996	0.135	0.668	−0.015	0.052
28.00	4855.406	0.000	3.542	−2.021	4.037	6.058	1.000	1.000	0.549	0.847	−0.066	0.040
28.00	4866.262	0.070	3.539	−1.991	3.820	5.811	1.000	1.000	0.475	0.827	−0.066	0.054
28.00	4873.438	−0.469	3.699	−1.955	4.282	6.237	0.995	1.000	0.334	0.781	−0.027	0.089
28.00	4904.407	−0.170	3.542	−2.013	4.146	6.159	0.994	1.000	0.518	0.837	−0.078	0.048
28.00	4913.968	−0.630	3.743	−2.029	4.234	6.263	0.976	0.999	0.215	0.735	−0.003	0.098
28.00	4918.362	−0.240	3.841	−1.961	4.299	6.260	1.000	1.000	0.365	0.796	−0.035	0.072
28.00	4935.831	−0.350	3.941	−2.141	4.110	6.251	0.989	1.000	0.181	0.749	−0.034	0.060
28.00	4976.320	−3.100	1.676	−2.020	4.375	6.395	1.000	1.000	0.341	0.626	−0.047	0.134
28.00	4980.166	−0.110	3.606	−1.966	4.354	6.320	1.000	1.000	0.591	0.847	−0.100	0.020
28.00	4984.112	0.350	3.796	−1.992	3.945	5.937	1.000	1.000	0.512	0.833	−0.089	0.021
28.00	4998.218	−0.780	3.606	−2.105	4.152	6.257	1.000	1.000	0.189	0.726	−0.024	0.082
28.00	5003.734	−2.800	1.676	−2.178	3.807	5.985	0.993	1.000	0.220	0.563	−0.036	0.152
28.00	5010.934	−0.870	3.635	−2.156	4.119	6.275	0.990	1.000	0.141	0.689	0.009	0.109
28.00	5017.568	−0.080	3.539	−2.079	4.110	6.189	1.000	1.000	0.539	0.842	−0.099	0.036
28.00	5035.357	0.290	3.635	−1.925	4.164	6.089	1.000	1.000	0.648	0.854	−0.168	−0.036
28.00	5042.182	−0.580	3.658	−2.079	4.164	6.243	1.000	1.000	0.248	0.754	0.000	0.095
28.00	5048.843	−0.380	3.847	−2.112	4.128	6.240	1.000	1.000	0.218	0.753	−0.118	0.000
28.00	5080.528	0.130	3.655	−1.960	4.321	6.281	1.000	1.000	0.637	0.853	−0.145	−0.021
28.00	5081.107	0.300	3.847	−1.953	4.212	6.165	0.999	1.000	0.574	0.838	−0.102	0.025
28.00	5082.339	−0.540	3.658	−2.075	4.170	6.245	0.999	0.999	0.268	0.761	−0.018	0.064
28.00	5084.089	0.030	3.679	−2.013	4.158	6.171	1.000	1.000	0.523	0.831	−0.091	0.030
28.00	5099.927	−0.100	3.679	−2.124	4.068	6.192	1.000	1.000	0.419	0.817	−0.054	0.066
28.00	5102.958	−2.620	1.676	−2.136	3.933	6.069	1.000	1.000	0.362	0.701	−0.027	0.131
28.00	5115.389	−0.110	3.834	−2.085	4.146	6.231	1.000	1.000	0.352	0.798	−0.036	0.070
28.00	5146.480	0.120	3.706	−2.068	3.968	6.036	0.989	1.000	0.463	0.819	−0.080	0.068
28.00	5155.762	−0.090	3.898	−2.127	4.110	6.237	0.989	1.000	0.308	0.788	−0.045	0.075
28.00	5176.559	−0.440	3.898	−2.241	3.993	6.234	1.000	1.000	0.133	0.711	−0.034	0.105
28.00	5424.642	−2.770	1.951	−2.086	4.240	6.326	0.996	0.999	0.267	0.605	−0.015	0.152
28.00	5435.855	−2.590	1.986	−2.147	4.234	6.381	0.997	1.000	0.328	0.692	−0.024	0.138
28.00	5578.711	−2.640	1.676	−2.175	3.957	6.132	1.000	0.999	0.361	0.696	−0.041	0.153
28.00	5587.853	−2.140	1.935	−2.133	3.872	6.005	1.000	1.000	0.403	0.727	−0.051	0.134
28.00	5589.357	−1.140	3.898	−1.963	4.312	6.275	0.987	1.000	0.061	0.407	0.040	0.144
28.00	5593.733	−0.840	3.898	−2.047	4.231	6.278	0.997	1.000	0.095	0.559	−0.015	0.000
28.00	5625.312	−0.700	4.089	−2.041	4.246	6.287	1.000	1.000	0.081	0.534	0.051	0.034
28.00	5682.198	−0.470	4.105	−2.114	4.182	6.296	1.000	1.000	0.104	0.624	0.000	0.085
28.00	5694.977	−0.610	4.089	−2.117	4.158	6.275	0.991	1.000	0.081	0.565	0.000	0.112
28.00	5748.346	−3.260	1.676	−2.048	4.203	6.251	1.000	1.000	0.194	0.428	−0.033	0.159
28.00	5754.655	−2.330	1.935	−2.056	4.347	6.403	1.000	1.000	0.542	0.762	−0.095	0.100
28.00	5805.213	−0.640	4.167	−1.999	4.300	6.299	1.000	1.000	0.083	0.525	0.006	0.100
28.00	5846.986	−3.210	1.676	−2.195	3.854	6.049	1.000	1.000	0.108	0.335	−0.001	0.199
28.00	6007.306	−3.330	1.676	−2.271	3.986	6.257	1.000	1.000	0.111	0.380	−0.005	0.184
28.00	6086.276	−0.530	4.266	−2.129	4.176	6.305	1.000	1.000	0.060	0.515	0.030	0.121
28.00	6108.107	−2.450	1.676	−2.093	4.036	6.129	1.000	1.000	0.491	0.719	−0.075	0.125
28.00	6128.963	−3.330	1.676	−2.247	4.010	6.257	1.000	0.996	0.113	0.387	−0.012	0.178
28.00	6175.360	−0.530	4.089	−2.095	4.204	6.299	1.000	1.000	0.101	0.583	−0.016	0.078
28.00	6176.807	−0.530	4.088	−2.102	4.405	6.507	1.000	1.000	0.150	0.646	−0.011	0.087
28.00	6191.171	−2.353	1.676	−2.061	4.113	6.174	1.000	1.000	0.561	0.741	−0.118	0.079
28.00	6314.653	−1.770	1.935	−2.234	3.522	5.756	1.000	0.998	0.399	0.714	−0.052	0.132
28.00	6327.593	−3.150	1.676	−2.120	4.164	6.284	1.000	1.000	0.217	0.496	−0.030	0.118
28.00	6482.796	−2.630	1.935	−2.115	3.924	6.039	0.965	0.994	0.197	0.500	−0.023	0.171
28.00	6532.871	−3.390	1.935	−1.969	4.300	6.269	1.000	1.000	0.094	0.230	−0.012	0.165
28.00	6586.308	−2.810	1.951	−2.144	4.110	6.254	1.000	0.995	0.187	0.507	−0.015	0.154

Table 2. continued.

Code (Fe I = 26.00)	λ (Å)	log gf	E_{low} (eV)	Δlog N $* - \odot$	log N (log N(H) = 12) Star	log N Sun	Blending (1 = clean line) Star	Blending Sun	Depth in synt. spectra Star	Depth in synt. spectra Sun	Error for log g +0.2	Error for T_{eff} +100 K
28.00	6643.629	−2.300	1.676	−1.865	4.387	6.252	1.000	1.000	0.631	0.736	−0.192	0.021
28.00	6767.768	−2.170	1.826	−2.023	4.234	6.257	1.000	1.000	0.570	0.728	−0.136	0.060
28.00	6772.313	−0.980	3.658	−2.026	4.270	6.296	1.000	1.000	0.131	0.549	−0.018	0.097
28.00	6914.559	−2.270	1.951	−2.055	4.164	6.219	1.000	1.000	0.444	0.672	−0.078	0.106
28.00	7122.191	0.040	3.542	−2.036	3.963	5.999	1.000	1.000	0.442	0.709	−0.087	0.046
28.00	7414.500	−2.570	1.986	−2.053	4.324	6.377	1.000	1.000	0.350	0.606	−0.054	0.126
28.00	7422.277	−0.140	3.635	−1.977	4.146	6.123	1.000	1.000	0.394	0.673	−0.075	0.058
28.00	7522.758	−0.575	3.658	−2.005	4.264	6.269	1.000	1.000	0.256	0.618	−0.033	0.088
28.00	7714.314	−2.200	1.935	−2.069	4.281	6.350	1.000	1.000	0.495	0.675	0.031	0.205
28.00	7727.613	−0.170	3.679	−1.982	4.134	6.116	1.000	1.000	0.350	0.647	−0.051	0.070
28.00	7748.891	−0.343	3.706	−2.023	4.270	6.293	1.000	1.000	0.324	0.643	−0.045	0.075
28.00	7788.936	−2.420	1.951	−1.926	4.510	6.436	1.000	1.000	0.493	0.645	−0.113	0.081
29.00	5105.528	−3.093	1.389	−2.817	1.317	4.134	0.154	0.454	0.029	0.331	−0.003	0.175
30.00	4722.153	−0.338	4.030	−1.777	2.678	4.455	0.997	1.000	0.552	0.785	−0.046	−0.073
30.00	4810.528	−0.137	4.078	−1.856	2.604	4.460	0.997	1.000	0.573	0.802	−0.055	−0.093
38.00	4607.327	0.302	0.000	−2.325	0.382	2.707	1.000	1.000	0.269	0.793	0.018	0.209
38.01	4161.792	−0.502	2.940	−2.217	0.722	2.939	0.972	0.994	0.165	0.603	−0.040	−0.144
39.01	4124.907	−1.500	0.409	−2.061	0.094	2.155	1.000	0.957	0.504	0.456	0.000	0.000
39.01	4854.863	−0.380	0.992	−2.076	−0.065	2.011	1.000	0.934	0.602	0.670	−0.022	−0.060
39.01	4883.684	0.070	1.084	−2.049	0.097	2.146	1.000	1.000	0.744	0.812	−0.161	−0.197
39.01	4900.120	−0.090	1.033	−2.060	0.054	2.114	1.000	1.000	0.717	0.784	−0.142	−0.181
39.01	4982.129	−1.290	1.033	−2.100	0.037	2.137	1.000	0.964	0.178	0.220	0.028	−0.010
39.01	5087.416	−0.170	1.084	−2.115	−0.023	2.092	1.000	0.999	0.642	0.728	−0.051	−0.088
39.01	5119.112	−1.360	0.992	−2.247	−0.015	2.232	1.000	0.911	0.153	0.246	0.064	0.055
39.01	5123.211	−0.830	0.992	−2.068	0.046	2.114	1.000	0.985	0.417	0.468	0.012	−0.018
39.01	5200.406	−0.570	0.992	−2.106	0.022	2.128	0.999	1.000	0.539	0.609	−0.014	−0.046
39.01	5205.724	−0.340	1.033	−2.146	0.014	2.160	1.000	1.000	0.613	0.702	−0.026	−0.058
39.01	5402.774	−0.510	1.839	−2.097	0.076	2.173	1.000	1.000	0.120	0.227	0.058	0.006
39.01	5509.895	−1.010	0.992	−2.107	0.005	2.112	1.000	0.974	0.294	0.353	0.053	0.017
39.01	5662.925	0.160	1.944	−2.125	0.200	2.325	0.964	0.933	0.371	0.576	0.023	−0.024
40.00	4687.809	0.550	0.730	−1.950	0.356	2.306	0.962	0.911	0.101	0.204	0.027	0.251
40.00	4739.480	0.230	0.651	−2.131	0.174	2.305	0.693	0.965	0.044	0.124	0.182	0.216
40.01	3998.954	−0.387	0.559	−2.161	0.390	2.551	1.000	1.000	0.810	0.878	−0.088	−0.067
40.01	4208.977	−0.460	0.713	−1.935	0.604	2.539	1.000	0.998	0.788	0.812	−0.132	−0.133
40.01	4161.213	−0.720	0.713	−2.328	0.548	2.876	0.999	1.000	0.706	0.835	−0.078	−0.063
40.01	4211.907	−1.083	0.527	−1.943	0.428	2.371	0.898	0.668	0.591	0.486	0.126	0.053
42.00	3864.104	−0.010	0.000	−2.472	−0.395	2.077	0.983	0.989	0.422	0.789	−0.001	0.131
56.01	5853.668	−1.000	0.604	−1.984	0.314	2.298	*hfs*	*hfs*	*hfs*	*hfs*	−0.266	−0.277
56.01	6141.730	−0.147	0.704	−2.263	0.440	2.703	*hfs*	*hfs*	*hfs*	*hfs*	−0.511	−0.503
56.01	6496.910	−0.427	0.604	−2.034	0.624	2.658	*hfs*	*hfs*	*hfs*	*hfs*	−0.500	−0.493
57.01	4086.709	−0.160	0.000	−1.953	−0.707	1.246	1.000	0.998	0.828	0.818	−0.179	−0.309
57.01	4322.503	−1.120	0.173	−1.901	−0.673	1.228	0.932	0.854	0.314	0.172	−0.003	−0.021
57.01	4662.498	−1.240	0.000	−1.804	−0.673	1.131	1.000	0.905	0.363	0.156	0.048	0.029
57.01	4740.276	−0.940	0.126	−1.916	−0.746		1.000		0.400		0.012	0.012

Table 2. continued.

Code (Fe I = 26.00)	λ (Å)	log gf	E_{low} (eV)	Δlog N $* - \odot$	log N (log N(H) = 12) Star	Sun	Blending (1 = clean line) Star	Sun	Depth in synt. spectra Star	Sun	Error for log g +0.2	Error for T_{eff} +100 K
57.01	4804.039	−1.500	0.235	−1.916	−0.746		0.989		0.114		0.006	0.006
57.01	4986.819	−1.210	0.173	−1.876	−0.706		1.000		0.245		0.027	0.012
57.01	5114.559	−1.060	0.235	−1.780	−0.610		1.000		0.330		0.038	0.031
57.01	5122.988	−0.930	0.321	−1.884	−0.591	1.293	1.000	0.991	0.346	0.211	0.021	0.024
57.01	5290.818	−1.750	0.000	−2.028	−0.818		0.978		0.109		0.100	0.084
57.01	5301.969	−1.000	0.403	−1.904	−0.734		1.000		0.199		0.064	0.037
57.01	5797.565	−1.410	0.244	−1.939	−0.646	1.293	1.000	0.955	0.158	0.091	0.012	0.012
57.01	6390.477	−1.450	0.321	−1.889	−0.658	1.231	1.000	0.999	0.118	0.061	0.071	0.045
58.01	3999.237	0.090	0.295	−1.994	−0.421	1.573	1.000	0.993	0.651	0.518	−0.018	−0.030
58.01	4042.580	0.180	0.495	−1.793	−0.392	1.401	1.000	1.000	0.578	0.336	0.012	−0.002
58.01	4068.836	−0.160	0.704	−1.872	−0.311	1.561	0.963	0.990	0.276	0.162	0.006	0.040
58.01	4073.474	0.230	0.478	−1.988	−0.421	1.567	1.000	0.968	0.597	0.487	0.057	0.048
58.01	4083.222	0.270	0.701	−1.982	−0.273	1.709	0.989	0.956	0.547	0.463	0.103	0.082
58.01	4118.143	0.190	0.696	−1.941	−0.330	1.611	0.989	0.885	0.466	0.351	0.024	0.025
58.01	4120.827	−0.210	0.320	−1.888	−0.385	1.503	0.981	0.877	0.483	0.272	0.040	0.063
58.01	4127.363	0.350	0.684	−1.821	−0.312	1.509	1.000	0.986	0.575	0.394	0.030	0.003
58.01	4137.645	0.440	0.517	−1.993	−0.379	1.614	0.994	0.997	0.701	0.635	−0.064	−0.030
58.01	4144.996	0.130	0.696	−1.845	−0.272	1.573	0.955	0.921	0.464	0.296	0.019	−0.077
58.01	4146.232	0.010	0.561	−1.745	−0.364	1.381	0.980	0.757	0.441	0.210	0.048	0.021
58.01	4193.102	−0.210	0.897	−1.886	−0.385	1.501	0.578	0.587	0.136	0.087	0.009	0.046
58.01	4193.871	−0.480	0.553	−1.961	−0.249	1.712	0.941	0.626	0.246	0.155	0.063	0.072
58.01	4202.958	−0.410	0.446	−2.091	−0.379	1.712	0.803	0.790	0.280	0.219	−0.006	−0.015
58.01	4222.597	0.020	0.122	−2.051	−0.597	1.454	0.997	0.994	0.642	0.501	−0.040	−0.015
58.01	4364.651	−0.230	0.495	−2.020	−0.528	1.492	0.869	0.705	0.265	0.184	0.033	0.038
58.01	4382.165	0.200	0.684	−1.937	−0.412	1.525	0.975	0.893	0.428	0.312	0.068	0.039
58.01	4391.659	0.050	0.322	−2.033	−0.453		0.913		0.590		−0.089	−0.004
58.01	4399.200	−0.380	0.327	−1.919	−0.346	1.573	0.999	1.000	0.396	0.216	0.018	0.028
58.01	4483.893	0.150	0.864	−1.964	−0.330	1.634	0.977	0.872	0.316	0.253	0.027	0.000
58.01	4486.909	−0.260	0.295	−1.899	−0.306	1.593	0.999	0.918	0.512	0.304	0.000	0.033
58.01	4523.075	−0.030	0.517	−1.890	−0.330	1.560	0.976	0.990	0.465	0.293	0.006	0.006
58.01	4539.745	−0.020	0.328	−1.807	−0.370	1.437	1.000	0.597	0.587	0.332	−0.006	−0.006
58.01	4560.958	−0.170	0.684	−1.781	−0.300	1.481	1.000	0.994	0.284	0.139	0.054	0.042
58.01	4562.358	0.230	0.478	−2.081	−0.476	1.605	1.000	0.999	0.560	0.502	0.006	−0.012
58.01	4582.498	−0.190	0.696	−1.745	−0.370	1.375	1.000	0.982	0.235	0.104	0.034	0.000
58.01	4593.925	0.110	0.696	−1.855	−0.238	1.617	0.990	1.000	0.463	0.294	0.017	−0.008
58.01	4606.400	−0.020	0.910	−1.956	−0.494	1.462	0.993	0.843	0.153	0.116	0.077	0.035
58.01	4628.161	0.200	0.517	−1.946	−0.430	1.516	1.000	0.987	0.538	0.399	0.006	−0.012
58.01	5187.458	0.150	1.212	−1.817	−0.343	1.474	0.923	0.800	0.134	0.091	0.013	0.037
58.01	5274.229	0.150	1.044	−2.023	−0.376	1.647	1.000	1.000	0.188	0.173	0.064	0.028
58.01	5330.556	−0.460	0.869	−2.010	−0.324	1.686	1.000	0.918	0.095	0.078	0.081	0.054
58.01	8025.570	−1.420	0.000	−1.931	−0.376	1.555	1.000	1.000	0.119	0.046	0.040	0.012
59.01	3908.428	0.156	0.000	−1.535	−0.924	0.611	0.989	0.910	0.766	0.343	−0.092	−0.098
59.01	4056.535	0.564	0.630	−1.355	−1.287	0.068	0.994	0.521	0.354	0.077	0.096	0.071
59.01	4179.393	0.310	0.204	−1.463	−0.753		0.988		0.770		−0.001	0.006
59.01	4408.819	0.018	0.000	−1.536	−0.826		1.000		0.734		−0.072	−0.081
59.01	5220.108	0.160	0.796	−1.679	−0.969		1.000		0.198		0.049	0.021
59.01	5259.728	0.080	0.633	−1.673	−1.112	0.561	0.996	0.970	0.197	0.077	0.063	0.029
59.01	5292.619	−0.300	0.648	−1.769	−1.059		1.000		0.096		0.074	0.047
59.01	5322.772	−0.315	0.483	−1.279	−0.895	0.384	1.000	0.709	0.203	0.030	0.037	0.033
59.01	5638.704	−1.116	0.630	−1.490	−0.780		0.904		0.033		0.006	0.018
59.01	5939.899	−0.088	1.244	−1.606	−0.896		1.000		0.044		0.091	0.031
59.01	6017.767	−0.257	1.112	−1.730	−0.950	0.780	1.000	1.000	0.038	0.020	0.079	0.040

Table 2. continued.

Code (Fe I = 26.00)	λ (Å)	log gf	E_{low} (eV)	Δlog N $*-\odot$	log N (log N(H) = 12) Star	log N (log N(H) = 12) Sun	Blending (1 = clean line) Star	Blending (1 = clean line) Sun	Depth in synt. spectra Star	Depth in synt. spectra Sun	Error for log g +0.2	Error for T_{eff} +100 K
60.01	3952.188	−0.540	0.000	−1.738	−0.183	1.555	1.000	0.941	0.769	0.457	−0.032	−0.045
60.01	4012.697	−0.740	0.000	−1.643	−0.130	1.513	1.000	0.973	0.710	0.305	−0.049	−0.061
60.01	4018.823	−0.890	0.064	−1.843	−0.377	1.466	1.000	0.975	0.437	0.185	0.021	−0.021
60.01	4021.327	0.230	0.321	−1.770	−0.765	1.005	0.988	0.974	0.671	0.394	−0.002	−0.001
60.01	4043.595	−0.510	0.321	−1.565	−0.424	1.141	0.979	0.640	0.440	0.123	−0.058	−0.159
60.01	4059.951	−0.360	0.205	−1.717	−0.549	1.168	1.000	1.000	0.538	0.218	−0.004	−0.016
60.01	4069.265	−0.390	0.064	−1.518	−0.347	1.171	0.999	0.891	0.729	0.276	−0.067	−0.063
60.01	4113.827	−0.900	0.182	−1.665	−0.166	1.499	1.000	0.808	0.465	0.154	0.026	0.023
60.01	4177.320	−0.080	0.064	−1.806	−0.449	1.357	1.000	0.939	0.790	0.595	−0.120	−0.128
60.01	4232.374	−0.300	0.064	−1.528	−0.379	1.149	1.000	0.935	0.744	0.312	−0.079	−0.061
60.01	4284.506	−0.162	0.631	−1.533	−0.363	1.170	0.976	0.797	0.441	0.145	0.075	0.042
60.01	4358.157	−0.123	0.321	−1.654	−0.233	1.421	1.000	0.937	0.732	0.432	−0.077	−0.067
60.01	4385.661	−0.540	0.205	−1.646	−0.120	1.526	0.999	0.941	0.672	0.312	−0.018	−0.006
60.01	4446.384	−0.590	0.205	−1.708	−0.120	1.588	1.000	1.000	0.640	0.316	−0.006	−0.006
60.01	4462.979	0.070	0.559	−1.453	−0.126	1.327	0.999	1.000	0.719	0.342	−0.086	−0.108
60.01	4465.595	−1.320	0.182	−1.721	−0.065	1.656	1.000	0.953	0.282	0.088	0.028	0.030
60.01	4516.346	−0.950	0.321	−1.499	−0.144	1.355	1.000	0.906	0.333	0.076	−0.018	0.018
60.01	4567.605	−1.510	0.205	−1.737	−0.203	1.534	1.000	0.938	0.142	0.042	0.041	0.044
60.01	4578.886	−1.060	0.321	−1.656	−0.212	1.444	1.000	0.903	0.246	0.073	0.083	0.086
60.01	4680.737	−1.260	0.064	−1.600	−0.171	1.429	1.000	0.811	0.331	0.079	0.045	0.036
60.01	4706.543	−0.880	0.000	−1.614	−0.114		1.000		0.627		−0.021	−0.012
60.01	4797.153	−0.950	0.559	−1.792	−0.239	1.553	1.000	0.948	0.164	0.071	0.098	0.068
60.01	4811.342	−1.140	0.064	−1.756	−0.014	1.742	1.000	0.954	0.495	0.196	0.077	0.050
60.01	4825.478	−0.860	0.182	−1.505	0.189	1.694	0.998	0.839	0.664	0.243	−0.044	−0.045
60.01	4859.026	−0.830	0.321	−1.690	0.123	1.813	1.000	0.656	0.555	0.249	0.010	−0.031
60.01	4914.382	−1.000	0.380	−1.675	−0.023	1.652	0.995	0.946	0.334	0.115	0.039	0.021
60.01	4943.899	−1.640	0.205	−1.641	−0.086	1.555	0.998	0.835	0.139	0.033	0.012	0.006
60.01	4947.020	−1.250	0.559	−1.792	−0.288	1.504	1.000	0.738	0.079	0.032	0.064	0.080
60.01	4961.387	−0.710	0.631	−1.692	−0.310	1.382	1.000	0.942	0.187	0.071	0.128	−0.007
60.01	4970.915	−1.650	0.321	−1.453	−0.126	1.327	1.000	0.595	0.091	0.015	0.000	0.000
60.01	4987.161	−0.830	0.742	−1.752	−0.292	1.460	0.982	0.976	0.117	0.051	0.051	0.022
60.01	4989.950	−0.500	0.631	−1.737	−0.467	1.270	1.000	0.834	0.205	0.088	0.051	0.033
60.01	4998.541	−1.100	0.471	−1.769	−0.358	1.411	1.000	0.838	0.117	0.044	0.051	0.057
60.01	5089.832	−1.160	0.205	−1.787	−0.347	1.440	0.993	0.996	0.213	0.075	0.046	0.049
60.01	5092.794	−0.610	0.380	−1.675	−0.347	1.328	1.000	1.000	0.366	0.129	0.028	0.015
60.01	5130.586	0.570	1.304	−1.788	−0.456	1.332	1.000	0.893	0.307	0.229	0.039	0.009
60.01	5132.328	−0.770	0.559	−1.855	−0.263	1.592	0.988	0.754	0.219	0.112	0.046	0.040
60.01	5212.361	−0.870	0.205	−1.605	−0.433	1.172	1.000	0.940	0.301	0.078	0.042	0.036
60.01	5221.572	−1.380	0.380	−1.712	−0.455	1.257	1.000	0.804	0.067	0.020	0.044	0.049
60.01	5234.194	−0.330	0.550	−1.656	−0.444	1.212	1.000	0.986	0.345	0.129	0.044	0.021
60.01	5249.576	0.210	0.976	−1.650	−0.264	1.386	1.000	0.951	0.439	0.234	0.028	−0.001
60.01	5255.506	−0.820	0.205	−1.602	−0.035	1.567	1.000	1.000	0.545	0.191	0.003	−0.009
60.01	5276.869	−0.440	0.859	−1.623	−0.567	1.056	1.000	0.874	0.107	0.038	0.062	0.036
60.01	5293.163	−0.060	0.823	−1.637	−0.165	1.472	1.000	0.993	0.446	0.219	0.021	−0.009
60.01	5311.453	−0.420	0.986	−1.698	−0.512	1.186	1.000	0.831	0.091	0.041	0.098	0.078
60.01	5319.815	−0.210	0.550	−1.578	−0.241	1.337	1.000	1.000	0.515	0.206	0.005	−0.020
60.01	5385.888	−0.820	0.742	−1.667	−0.336	1.331	0.999	0.873	0.109	0.038	0.075	0.052
60.01	5421.551	−1.330	0.380	−1.461	−0.254	1.207	0.998	0.599	0.118	0.020	0.077	0.062
60.01	5431.516	−0.400	1.121	−1.634	−0.259	1.375	1.000	0.922	0.109	0.048	0.079	0.040
60.01	5442.264	−0.910	0.680	−1.640	−0.324	1.316	1.000	0.769	0.108	0.035	0.071	0.052
60.01	5688.518	−0.250	0.986	−1.809	−0.408	1.401	0.982	0.785	0.159	0.093	0.070	0.033
62.01	3793.978	−0.635	0.104	−1.701	−0.730	0.971	0.988	0.513	0.477	0.165	0.116	0.071
62.01	3896.972	−0.576	0.040	−1.513	−0.732	0.781	0.983	0.710	0.559	0.143	−0.019	0.020

Table 2. continued.

Code (Fe I = 26.00)	λ (Å)	log gf	E_{low} (eV)	Δlog N $*-\odot$	log N (log N(H) = 12) Star	log N (log N(H) = 12) Sun	Blending (1 = clean line) Star	Blending (1 = clean line) Sun	Depth in synt. spectra Star	Depth in synt. spectra Sun	Error for log g +0.2	Error for T_{eff} +100 K
62.01	3993.309	−0.876	0.040	−1.692	−0.565	1.127	1.000	0.924	0.474	0.158	0.020	0.012
62.01	4206.124	−0.931	0.378	−1.548	−0.612	0.936	0.941	0.568	0.196	0.046	0.048	−0.101
62.01	4256.391	−0.447	0.378	−1.666	−0.446	1.220	0.976	0.948	0.538	0.233	0.040	0.040
62.01	4318.927	−0.613	0.277	−1.680	−0.408	1.272	0.998	0.967	0.537	0.226	0.010	−0.003
62.01	4452.722	−0.823	0.277	−1.514	−0.287	1.227	0.986	0.720	0.482	0.135	0.036	0.018
62.01	4467.341	−0.300	0.659	−1.505	−0.127	1.378	1.000	0.958	0.581	0.247	−0.002	−0.025
62.01	4519.630	−0.751	0.544	−1.611	−0.474	1.137	0.891	0.814	0.235	0.075	0.064	0.051
62.01	4577.688	−1.234	0.248	−1.611	−0.257	1.354	0.979	0.663	0.288	0.078	0.075	0.063
62.01	4606.510	−1.359	0.000	−1.639	−0.505	1.134	1.000	0.966	0.259	0.063	0.056	0.062
62.01	4777.840	−1.285	0.040	−1.458	−0.574	0.884	1.000	0.978	0.236	0.039	−0.069	−0.070
63.01	3907.099	−1.442	0.207	−1.736	−1.156	0.580	*hfs*	*hfs*	*hfs*	*hfs*	0.044	0.030
63.01	4129.735	−0.843	0.000	−1.364	−0.939	0.425	*hfs*	*hfs*	*hfs*	*hfs*	−0.020	0.012
63.01	4205.058	−0.871	0.000	−1.656	−0.920	0.736	*hfs*	*hfs*	*hfs*	*hfs*	0.007	0.009
63.01	6437.640	−2.429	1.320	−1.502	−0.606	0.896	*hfs*	*hfs*	*hfs*	*hfs*	0.086	0.043
63.01	6645.063	−0.791	1.380	−1.399	−0.899	0.500	*hfs*	*hfs*	*hfs*	*hfs*	0.277	0.294
63.01	7301.194	−2.138	1.250	−1.585	−1.026	0.559	*hfs*	*hfs*	*hfs*	*hfs*	0.075	0.018
64.01	4049.855	0.429	0.991	−1.669	−0.564	1.105	1.000	0.994	0.425	0.254	0.013	−0.052
64.01	4085.558	−0.009	0.731	−1.593	−0.459	1.134	1.000	0.911	0.425	0.184	0.111	0.070
64.01	4130.366	0.139	0.731	−1.534	−0.414		1.000		0.533		−0.004	−0.030
64.01	4251.731	−0.365	0.382	−1.757	−0.456	1.301	0.999	0.839	0.481	0.244	−0.006	0.006
64.01	4483.329	−0.662	1.060	−1.442	−0.053	1.389	1.000	0.869	0.126	0.040	0.048	0.015
66.01	3694.810	−0.110	0.103	−1.218	−0.187	1.031	1.000	0.912	0.871	0.579	−0.211	−0.275
66.01	3983.651	−0.252	0.538	−1.371	−0.335	1.036	1.000	0.884	0.628	0.233	−0.030	−0.047
66.01	3996.689	−0.207	0.590	−1.343	−0.294	1.049	1.000	0.974	0.637	0.237	0.037	0.022
66.01	4073.121	−0.097	0.538	−1.325	−0.512	0.813	0.998	0.895	0.619	0.203	0.172	−0.063
66.01	4103.310	−0.376	0.103	−1.100	−0.075	1.025	1.000	0.692	0.836	0.386	−0.079	−0.100
66.01	4449.700	−1.029	0.000	−1.325	−0.277	1.048	1.000	1.000	0.607	0.140	−0.017	−0.015
66.01	4468.140	−1.665	0.103	−1.664	−0.312	1.352	0.967	0.845	0.185	0.056	0.113	0.139
68.01	4500.751	0.037	1.816	−1.365	−0.459	0.906	0.934	0.717	0.069	0.034	0.065	0.041
68.01	4759.653	−1.904	0.000	−1.446	−0.394	1.052	0.979	0.702	0.163	0.029	0.018	0.033
69.01	3848.020	−0.100	0.000	−1.153	−1.319	−0.166	1.000	0.522	0.742	0.181	−0.080	−0.089
72.01	3918.094	−1.010	0.452	−0.966	−0.075	0.891	0.999	0.976	0.736	0.136	0.004	−0.027
72.01	4093.155	−1.090	0.452	−1.487	−0.837	0.650	1.000	0.526	0.270	0.068	0.217	0.198
74.00	4008.749	−0.427	0.366	−1.516	−0.573	0.943	0.864	0.681	0.340	0.105	−0.083	−0.086
74.00	4074.357	−0.708	0.366	−1.871	−0.761		0.557		0.142		−0.124	0.239
76.00	4112.011	−1.310	0.715	−1.136	0.314		0.968		0.237		−0.168	−0.039
76.00	4135.775	−1.350[a]	0.516	−1.081	0.279		0.935		0.380		−0.380	−0.169
76.00	4260.848	−1.470[a]	0.000	−1.429	−0.009		1.000		0.511		−0.016	0.195
76.00	4420.468	−1.530	0.000	−1.276	0.072	1.348	0.995	0.852	0.506	0.086	0.159	0.358
77.00	3800.120	−1.489[a]	0.000	−1.180	0.131		1.000		0.755		0.064	0.076
82.00	4057.806	−0.176	1.320	−1.848	0.123	1.971	0.974	0.920	0.176	0.385	−0.019	0.244
90.01	4003.309	−0.760	1.141	−1.100	−1.010		0.872		0.029		−0.036	0.000
90.01	4019.129	−0.228[b]	0.000	−1.373	−1.283		0.997		0.643		0.027	0.012

Table 2. continued.

Code (Fe I = 26.00)	λ (Å)	log gf	E_{low} (eV)	Δlog N $*-\odot$	log N (log N(H) = 12) Star	Sun	Blending (1 = clean line) Star	Sun	Depth in synt. spectra Star	Sun	Error for log g +0.2	Error for T_{eff} +100 K
90.01	4086.521	−0.929[b]	0.000	−1.429	−1.339		0.981		0.216		−0.002	−0.019
90.01	4094.747	−0.885[b]	0.000	−1.149	−1.059		0.957		0.378		0.020	0.048
90.01	4178.060	−0.649	0.909	−1.070	−0.980		0.579		0.074		0.132	0.011
90.01	4179.714	−1.330[b]	0.189	−1.211	−1.121		0.824		0.091		0.047	0.071
90.01	5989.045	−1.414[b]	0.189	−1.167	−1.077		0.999		0.086		0.082	0.067
92.01	3854.640	0.124	0.578	<−0.968	<−1.438		0.926		0.318			
92.01	3865.917	−0.421[b]	0.285	<−1.797	<−2.267		0.634		0.041			
92.01	3890.361	−0.467	0.036	<−1.068	<−1.538		0.753		0.315			
92.01	4044.412	−0.554	0.652	<−1.799	<−2.269		0.116		0.011			
92.01	4050.041	−0.706[b]	0.000	<−1.323	<−1.793		0.928		0.135			
92.01	4090.132	−0.184[b]	0.217	<−1.358	<−1.828		0.991		0.204			
92.01	4171.588	−0.474[b]	0.217	<−1.495	<−1.965		0.571		0.085			
92.01	4341.683	−0.700[b]	0.036	<−1.765	<−2.235		0.218		0.048			

[a] log gf from Ivarsson et al. (2003), A&A, 409, 1141.
[b] log gf from Nillson et al. (2002), A&A, 382, 368 and Nillson et al. (2002), A&A, 381, 1090.